Aprotinin prevents proteolytic ENaC activation and volume retention in nephrotic syndrome

Bernhard N. Bohnert[1-3*], Martina Menacher[1*], Andrea Janessa[1], Matthias Wörn[1], Anja Schork[1-3], Sophie Daiminger[1], Hubert Kalbacher[4], Hans-Ulrich Häring[1-3], Christoph Daniel[5], Kerstin Amann[5], Florian Sure[6], Marko Bertog[6], Silke Haerteis[6], Christoph Korbmacher[6], Ferruh Artunc[1-3]

* Shared first authorship

[1] Department of Internal Medicine, Division of Endocrinology, Diabetology, Vascular Disease, Nephrology and Clinical Chemistry, University Hospital Tübingen, Germany

[2] Institute of Diabetes Research and Metabolic Diseases (IDM) of the Helmholtz Center Munich at the University Tübingen, Germany.

[3] German Center for Diabetes Research (DZD) at the University Tübingen, Germany.

[4] Interfacultary Institute of Biochemistry, University Tübingen, Germany

[5] Institute of Pathology, Friedrich-Alexander University Erlangen-Nürnberg (FAU), Erlangen, Germany

[6] Institute of Cellular and Molecular Physiology, Friedrich-Alexander University Erlangen-Nürnberg (FAU), Erlangen, Germany

Address for correspondence:

Ferruh Artunc, MD
Department of Internal Medicine
Division of Endocrinology, Diabetology, Angiology and Nephrology
University Hospital of Tübingen
Otfried-Mueller-Str.10
72076 Tübingen, Germany
E-mail: ferruh.artunc@med.uni-tuebingen.de
Tel. +49-7071-2982711
Fax +49-7071-2925215

Running head: aprotinin and nephrotic syndrome

Key words: nephrotic syndrome – aprotinin - mice – ENaC - serine protease – proteolysis – protease inhibitor - proteolytic channel activation

Abstract

Volume retention in nephrotic syndrome has been linked to activation of the epithelial sodium channel (ENaC) by proteolysis of its γ-subunit following urinary excretion of serine proteases such as plasmin. We hypothesized that pharmacological inhibition of urinary serine protease activity might protect from ENaC activation and volume retention in nephrotic syndrome. Here we show that urine from both nephrotic mice (induced by doxorubicin injection) and nephrotic humans display high aprotinin-sensitive serine protease activity. Treatment of nephrotic mice with the serine protease inhibitor aprotinin delivered by subcutaneous sustained release pellets normalized urinary serine protease activity and prevented sodium retention as did treatment with the ENaC inhibitor amiloride. In kidney cortex from nephrotic mice, immunofluorescence revealed increased apical γ-ENaC staining that was normalized by aprotinin treatment. In *Xenopus laevis* oocytes heterologously expressing murine ENaC, aprotinin had no direct inhibitory effect on channel activity but prevented proteolytic channel activation. In conclusion, this study shows that volume retention in experimental nephrotic syndrome is related to proteolytic ENaC activation by proteasuria and can be prevented by treatment with aprotinin. Inhibition of urinary serine protease activity might become a new therapeutic approach to treat patients with nephrotic-range proteinuria.

Introduction

Nephrotic syndrome is characterized by proteinuria, edema, hypoalbuminemia, and hyperlipidemia, and it represents the most severe manifestation of proteinuric renal disease. The pathogenesis of edema formation in nephrotic syndrome remains debatable, and both underfill and overfill theories have been proposed [1]. Studies of nephrotic rats have suggested that the distal tubule expressing the epithelial sodium channel (ENaC) is the site of sodium retention [2]. In addition to regulation by the mineralocorticoid hormone aldosterone [3], a special feature of ENaC is its complex post-translational regulation by proteases which cleave specific sites in the extracellular domains of the α- and γ-subunit [4]. Recent evidence suggests that proteolytic ENaC activation by urinary proteases may contribute to sodium retention in nephrotic syndrome [5, 6]. Protein-rich urine samples from both nephrotic rats [7] and patients [8] have been shown to activate ENaC currents *in vitro*, which is thought to be the result of proteolysis of the γ-subunit of ENaC by serine proteases excreted in the urine [9]. Currently, the serine protease plasmin has been implicated in promoting ENaC activation and volume retention during proteinuria [7, 10]. Plasmin cleaves the γ-subunit of ENaC at a distinct site and induces a robust increase in ENaC currents *in vitro* [10, 11]. In humans, a close correlation of urinary plasmin excretion with proteinuria has been shown in preeclampsia [8] and diabetic nephropathy [12, 13]. We have found a strong association of plasminuria with overhydration determined from bioimpedance spectroscopy in a large sample of chronic kidney disease (CKD) patients [14].

Targeting urinary plasmin activity by pharmacological inhibitors may be an interesting therapeutic approach given the putative role of plasminuria in mediating volume retention and possibly podocyte injury [15]. Plasmin can be inhibited by the serine protease inhibitor aprotinin that competitively interacts with its catalytic site and by tranexamic acid that inhibits plasminogen conversion into plasmin after occupying lysine-binding sites at the kringle domains of plasminogen. Camostat is an orally available serine protease inhibitor with activity

against plasmin that was originally developed in Japan for the treatment of pancreatitis. Anecdotal reports suggest that camostat has beneficial effects in nephrotic patients [16, 17]. Camostat has also been reported to reduce blood pressure in salt-sensitive hypertensive rats, probably by preventing proteolytic ENaC activation as suggested by the detection of partially but not fully cleaved γENaC [18, 19]. The inhibition of urinary plasmin activity requires the availability of these drugs in the tubular fluid. Aprotinin as a small polypeptide with 58 amino acids (6.5 kDa) and tranexamic acid as a water-soluble organic acid are eliminated exclusively *via* glomerular filtration. Camostat is rapidly degraded by plasmatic esterases into two metabolites that are excreted in the urine, of which one has preserved inhibitory activity [20]. Therefore, these drugs which have negligible plasma protein binding can reach therapeutically relevant concentrations in the tubular fluid, which makes them candidates for a pharmacological intervention to inhibit tubular protease activity in experimental nephrotic syndrome. In rats with experimental heart failure that developed plasminuria, aprotinin treatment resulted in a blunted response to ENaC blockade by benzamil suggestive of reduced ENaC activity [21].

In this study, we tested the hypothesis that pharmacological inhibition of urinary serine protease activity *in vivo* may reduce volume retention in nephrotic mice. Therefore, we used the inhibitors aprotinin, camostat, and tranexamic acid and tested their effect on volume retention in a model of experimental nephrotic syndrome developed by our group [22, 23]. We show that aprotinin treatment abolishes volume retention by preventing proteolytic ENaC activation.

Results

Experimental nephrotic syndrome in mice features all hallmarks of human nephrotic syndrome.

Following a single injection of doxorubicin, mice with proteinuria exceeding 140 mg/mg crea developed nephrotic syndrome characterized by hypoalbuminemia (Fig. 1A), body weight gain with ascites (Fig. 1B, Suppl. Fig 1A), and hyperlipidemia evidenced by lipemic plasma (Suppl. Fig. 1B). Although food and fluid intake remained fairly constant, except for a modest decrease during the initial days after doxorubicin treatment (Suppl. Fig. 1C), urinary sodium/creatinine and urinary Na/K ratio dropped dramatically during the first 10 days, indicating that sodium retention caused the body weight gain (Fig. 1B, Suppl. Fig. 1D). Urinary activity to cleave the amide bond of the chromogenic substrate S-2251 increased and was paralleled by a 1000-fold increase in urinary plasmin(ogen) excretion as measured using ELISA and fall in plasma plasmin(ogen) concentration (Fig. 1C).

Urinary amidolytic activity could be competitively inhibited *in vitro* by the serine protease inhibitors aprotinin (IC_{50} 56 [23; 137] nM) and camostat (IC_{50} 2.4 [1.1; 4.9] µM) but not by tranexamic acid (Fig. 1D). Urinary amidolytic activity was also sensitive to inhibition by anti-plasmin (IC_{50} 51 [40; 66] nM) indicating that plasmin activity accounted for the vast proportion of urinary amidolytic activity against S-2251. Similar inhibition curves were obtained when amidolytic activity of purified plasmin was analyzed (Suppl. Fig. 2). IC_{50} values were not significantly different (Suppl. Table 1), except for camostat (IC_{50} 0.4 [0.4; 0.5] µM, p=0.0003).

Patients with nephrotic syndrome display aprotinin-sensitive urinary serine protease activity.

In ten patients with acute nephrotic syndrome and nephrotic-range proteinuria as characterized in supplemental table 2 and by Schork et al. [14], we detected strong urinary amidolytic activity that was almost absent in fifteen healthy subjects (Fig. 2A/B, Suppl. table 2). In nephrotic patients, this activity was largely sensitive to aprotinin and accounted for 73 ± 7 % of total

activity whereas this proportion was only 10 ± 3% in healthy subjects ($p<0.0001$). The increased urinary amidolytic activity in the nephrotic patients paralleled the expansion of extracellular volume as quantified by bioimpedance spectroscopy (Fig. 2C, Suppl. table 2). These findings confirm that nephrotic syndrome in both humans and mice leads to excretion of urinary serine proteases that might be involved in volume retention.

Treatment of nephrotic mice with aprotinin prevents volume retention.

To test the effect of pharmacological inhibition of urinary serine protease activity *in vivo* we treated nephrotic mice with aprotinin, camostat or tranexamic acid delivered by sustained release pellets. After induction of nephrotic syndrome, we implanted the pellets subcutaneously on day 3 and followed nephrotic mice until day 10. Nephrotic mice receiving placebo pellets served as controls. After induction of nephrotic syndrome, proteinuria (Fig. 3A) as well as food and fluid intake was similar in all treatment groups (Suppl. Fig. 3A/B). Urinary amidolytic activity was suppressed by aprotinin but not by camostat or tranexamic acid (Fig. 3B). While camostat and tranexamic acid-treated mice showed similar body weight gain as placebo-treated nephrotic mice, aprotinin-treated nephrotic mice were protected (Fig. 3C). Accordingly, urinary sodium/creatinine ratio was normalized in aprotinin-treated nephrotic mice compared to the other groups (Fig. 3D, Suppl. Fig. 3C). Treatment with aprotinin prevented the reduction in plasma sodium concentration seen in the other nephrotic groups (table 1). Compared to healthy mice, nephrotic mice of all groups tended to have higher plasma potassium concentrations and were hypoalbuminemic (table 1). Glomerular filtration rate as estimated from plasma urea and creatinine concentration showed mild reductions in nephrotic mice, reaching statistical significance in mice treated with tranexamic acid (table 1).

Urinary and plasma aprotinin concentrations under treatment with 1 mg of aprotinin per day are shown in Fig. 3E. Mean urinary aprotinin concentration was 443 ± 90 µg/ml (68 ± 13 µM)

whereas plasma aprotinin concentration after 10 days of treatment was 14 ± 2 µg/ml (2.1 ± 0.3 µM), which is comparable to the plasma concentration achieved in aprotinin-treated patients [24]. Dose response studies with different aprotinin doses showed that 0.5 mg partially and 1 mg per day completely prevented body weight gain, although the urinary amidolytic activities (both *in vitro* and *in vivo*) were inhibited by lower doses such as 0.25 and 0.5 mg per day (Fig. 3F). Similar effects as those with aprotinin were obtained after treatment with the ENaC blocker amiloride, which also prevented sodium retention and body weight gain in nephrotic mice (Fig. 4A-C). This confirms the concept that increased ENaC-mediated sodium absorption plays a major role in volume retention in nephrotic syndrome and suggests that the therapeutic effect of aprotinin is mediated by inhibiting proteolytic ENaC activation by urinary serine proteases.

Plasma aldosterone is reduced by aprotinin and is not essential for volume retention.

Compared to healthy mice, plasma aldosterone concentrations were increased in nephrotic mice on placebo treatment but not in nephrotic mice treated with aprotinin, camostat or tranexamic acid (Fig. 4D). To dissect the contribution of hyperaldosteronism and to exclude the possibility that the effect of aprotinin was due to prevention of hyperaldosteronism, we studied the volume retention under suppressed aldosterone secretion and mineralocorticoid receptor (MR) blockade. Compared to nephrotic mice on a normal diet, body weight gain was significantly higher under high salt intake despite suppressed aldosterone plasma concentration (+33.0 ± 6.4 %). Still, aprotinin treatment inhibited volume retention in mice with high-salt intake (Suppl. Fig. 4A). Treatment with the MR blocker potassium canrenoate did not prevent volume retention, although the increase tended to be slightly blunted (+15.9 ± 3.3%, Fig. 4A-C). As shown in Suppl. Fig. 4B, maximal body weight gain did not parallel plasma aldosterone concentration during various treatments arguing against a major and causal contribution of aldosterone to the observed volume retention. Quantitative PCR revealed that nephrotic mice

had significantly increased transcript levels of renin compared to healthy mice whereas renin transcript levels were suppressed in aprotinin- treated nephrotic mice (Fig. 4E). The results were robust when mRNA transcript levels were expressed in absolute copies or normalized to β-actin (Suppl. Fig. 5A/B). GAPDH was significantly less expressed in aprotinin-treated nephrotic mice and could therefore not be used for normalization (Suppl. Fig. 5C).

Aprotinin treatment affects expression of γ-ENaC and its cleavage products.

Compared to healthy mice, mRNA expression of the α-, β-, and γ-subunits of ENaC tended to decrease in placebo-treated nephrotic mice reaching statistical significance in aprotinin-treated nephrotic mice (Fig. 5A, Suppl. Fig. 6A-B). Analysis of the γ-ENaC expression in renal cortical tissue by Western blotting using a C-terminal mouse γ-ENaC antibody showed multiple bands at 44, 53, 70, 76 and 86 kDa that were blocked by the application of the immunogenic peptide (Fig. 5B). Linearity of the signal intensity was confirmed with different loading (Suppl. Fig. 7A/B). The strongest band among these was the one at 70 kDa most likely representing furin-cleaved γ-ENaC at the plasma membrane while the 86 kDa band represented full-length γ-ENaC (Fig. 5C). However, a specific band representing extracellularly cleaved γ-ENaC which is expected to be 5 kDa smaller than furin-cleaved γ-ENaC was not detectable. Compared to healthy mice, the expression of the bands at 53, 70, 76 and 86 kDa was significantly decreased in placebo-treated nephrotic mice. A similar pattern was observed in aprotinin-treated nephrotic mice, however, the band at 53 kDa was significantly decreased compared to healthy and placebo-treated nephrotic mice (Fig. 5E).

Histological analysis of renal tissue showed up-regulation of γ-ENaC staining in placebo-treated nephrotic mice (Fig. 6), resulting in a significantly higher staining score compared to healthy mice (1.8 ± 0.03 vs. 0.9 ± 0.04, p=0.0004, Suppl. Fig 8A). At higher magnification, increased staining was particularly observed at the luminal side of the principal cells, a finding

similar to what has previously been described in nephrotic rats and referred to as apical targeting of ENaC [25]. Aprotinin treatment normalized γ-ENaC staining (0.8 ± 0.1) and prevented apical targeting. γ-ENaC staining was negative in the presence of the blocking peptide (Suppl. Fig. 8B).

Aprotinin has no inhibitory effect on ENaC activity and prevents the appearance of a γ-ENaC cleavage product at 67 kDa in X.laevis oocytes.

Based on the similar efficacy of the ENaC blocker amiloride and the serine protease inhibitor aprotinin, we further analyzed the mode of action of aprotinin by studying its effect on murine ENaC heterologously expressed in *Xenopus laevis* oocytes. As shown in Fig. 7A/C, application of 500 µg/ml aprotinin – a concentration achieved in the urine of aprotinin-treated nephrotic mice – to the bath solution did not markedly affect ENaC-mediated currents (ΔI_{ami}). The minor current rundown observed with aprotinin was similar to that observed in time-matched control experiments with mock solution exchange (Fig. 7B/C). These results exclude a relevant direct inhibitory effect of aprotinin on ENaC.

In additional control experiments the prototypical serine protease chymotrypsin (2 µg/ml) increased amiloride-sensitive ENaC-mediated whole-cell currents by about 2-fold (Suppl. Fig. 9A). In this concentration chymotrypsin has been shown to fully activate ENaC by cleaving the channel at a specific site in its γ-subunit. [11]. Subsequent addition of 500 µg/ml aprotinin to the chymotrypsin containing solution did not affect ΔI_{ami} (Suppl. Fig. 9B). Importantly, application of chymotrypsin in the presence of aprotinin failed to stimulate ENaC currents, whereas subsequent removal of aprotinin in the continuous presence of chymotrypsin revealed the expected ~2-fold proteolytic ENaC activation (Suppl. Fig. 9C). In parallel Western blots assessing biotinylated cell surface expressed γ-ENaC (Fig. 7D), a predominant cleavage product of ~76 kDa was detectable in oocytes expressing αβγ-ENaC. In the oocyte system full-

length mouse γ-ENaC migrates at ~87 kDa and is readily detectable in whole-cell lysate or in membrane-enriched fractions but usually not at the cell surface [7, 11, 26]. This indicates that γ-ENaC detected at the plasma membrane is pre-cleaved at amino acid position 143 by the endogenous serine protease furin which is not sensitive to aprotinin [27] (Fig. 5C). As expected, ENaC activation by chymotrypsin treatment induced a shift of the molecular size of cell surface expressed γ-ENaC from 76 to 67 kDa (Fig. 5C). This supports the concept that a second cleavage event in γ-ENaC is required as a final step in proteolytic channel activation [11]. The appearance of the ~67 kDa cleavage fragment was prevented when chymotrypsin was applied in the presence of aprotinin (Fig. 7D) consistent with the finding that aprotinin prevented the activation of ENaC currents by chymotrypsin (Suppl. Fig. 9C). Aprotinin treatment alone had no effect on the appearance of the ~76 kDa fragment. We also tested the long-term effect of aprotinin on ENaC currents. Pre-incubation of murine ENaC expressing oocytes for 48 h in aprotinin had no significant effect on baseline ΔI_{ami} and did not alter the relative stimulatory effect of chymotrypsin (Suppl. Fig. 9D).

Discussion

This study is the first to demonstrate the pathophysiological role of urinary serine protease activity and proteolytic ENaC activation for volume retention in an *in vivo* model of experimental nephrotic syndrome. It highlights that treatment with the serine protease inhibitor aprotinin abolished ENaC-mediated sodium retention by preventing proteolytic ENaC activation. However, it is unclear whether this is related to inhibition of plasmin or whether other aprotinin-sensitive serine proteases contribute to or mediate this effect. These might include membrane-anchored prostasin and tissue kallikreins that are involved in the physiological regulation of ENaC [28, 29] as well as serine proteases of the coagulation cascade that are aberrantly filtered during proteinuric disease. It is also unclear whether complex serine proteases cascades are involved in proteolytic ENaC activation. For example, plasmin has been shown to potentially activate ENaC by direct cleavage at a distinct site [11] or to activate prostasin that subsequently cleaves γ-ENaC at the putative prostasin site [30]. Aprotinin also inhibits prostasin with high affinity (IC_{50} 1.8 nM [31]), and thus, the efficacy of aprotinin may result from the inhibition of both pathways. Further studies are needed to elucidate the complex mechanisms of proteolytic ENaC activation during nephrotic syndrome and the effect of aprotinin.

In our study, patients with acute nephrotic syndrome as well as nephrotic mice showed volume retention and excretion of aprotinin-sensitive serine proteases in the urine which can be termed proteasuria. This finding suggests common mechanisms in ENaC activation of nephrotic patients and the current nephrotic mouse model supporting its validity to study human disease. Currently, plasmin is suggested to be the principal serine protease involved in ENaC-mediated sodium retention in nephrotic syndrome [5, 7]. However, there is still the possibility that aprotinin-sensitive serine proteases other than plasmin might also be involved. Our findings are a proof of principle that the inhibition of urinary serine protease activity might become a new

therapeutic approach that may be translated into clinical medicine to treat nephrotic patients. Compared to direct ENaC blockade with the diuretic amiloride, the inhibition of excessive urinary serine protease activity could protect from ENaC-mediated volume retention while minimally interfering with basal ENaC function. Therefore, it might confer protection from the development of life-threatening hyperkalemia, which limits amiloride treatment in clinical practice, particularly in patients with renal insufficiency [32-35]. Notably, plasma potassium concentration was not increased in aprotinin-treated nephrotic mice compared to placebo-treated nephrotic mice. Although effective in this study, aprotinin might not be an ideal drug for the treatment of patients given its side effects of which renal events also have been described [36].

Western blots from mouse kidneys and oocytes expressing murine ENaC showed distinct differences in the expression of the γ-ENaC cleavage products. In plasma membranes from oocytes, γ-ENaC was only expressed at 76 kDa, and the addition of chymotrypsin induced a shift to 67 kDa corresponding to extracellularly cleaved γ-ENaC. In contrast, healthy mice expressed multiple bands under control conditions from which the ones at 86 and 70 kDa probably represented full-length and furin-cleaved γ-ENaC, respectively. Although the appearance of serine proteases is expected to result in proteolytic activation of γ-ENaC *in vivo*, we could not clearly detect a band with the expected size that could represent extracellularly cleaved γ-ENaC except for a band at 53 kDa that was attenuated by aprotinin treatment. However, it has not been shown that γ-ENaC fragments lower than 65 kDa represent proteolytically activated ENaC. In similar Western blots analyses from mouse kidney homogenates using an analogous antibody directed against the corresponding C-terminal γ-ENaC sequence from rat, Yang et al. detected bands at 80, 70 and 65 kDa with the latter supposed to represent extracellularly cleaved γ-ENaC [37]. The difference in molecular weight of this γ-ENaC cleavage product between our and that study is unclear and might be related to

differences in one of the five N-glycosylation sites [38], sample preparation and the antibody used. Also fluorescence detection using infrared dye-labelled antibodies is by far more sensitive than commonly employed chemiluminescence detection. A limitation of Western blots analyses from whole kidney homogenates to assess ion channels is its inherent difficulty to distinguish between cell-surface and intracellularly expressed ion channels. To overcome this, the group of Palmer et al. has developed a protocol to analyze cell-surface expressed ENaC by an *in vivo* biotinylation approach [39, 40]. While this has been successfully implemented in rats, we chose to enrich membrane proteins by ultracentrifugation. We also employed a blocking peptide to dissect unspecific bands which were seen at 48 and 65 kDa. With this respect, histological analysis is more suitable to analyze the expression of functionally active channels at the plasma membrane. Immunofluorescene showed marked up-regulation of γ-ENaC staining, particularly at the apical side, in placebo-treated nephrotic mice that might relate to increased apical targeting due to hyperaldosteronism [25, 41]. Aprotinin inhibited apical targeting, most likely by suppression of hyperaldosteronism. Due to the used antibody, immunofluorescence does not allow any inference about γ-ENaC proteolysis.

Our electrophysiological data using mouse ENaC expressing oocytes clearly show that aprotinin does not exert a direct inhibitory effect on ENaC *in vitro* but prevents its proteolytic activation and the appearance of the 67 kDa γ-ENaC cleavage fragment representing the fully active channel. This is in good agreement with previous findings from Carattino et al. [28] in ENaC expressing oocytes and also fit to the results reported by Jacquillet et al.[42] showing that aprotinin abolished the stimulatory effect of chymotrypsin on sodium reabsorption *in vivo*, while aprotinin alone had no effect.

Although activation of renin and aldosterone secretion was suppressed in all mice treated with serine protease inhibitors, only aprotinin-treated mice were protected from the increase in amidolytic activity and volume retention. This could be explained with insufficient delivery of

camostat and tranexamic acid to the distal tubule. A study with radiolabeled camostat has demonstrated that only 12% of the radioactivity found in the urine corresponded to the active metabolite GBPA [20].

Our findings support the overfill hypothesis of sodium retention during nephrotic syndrome in several aspects. First, the onset of sodium retention was immediately after the occurrence of proteinuria. Second, proteinuria had to be in excess of a threshold of approximately >140 mg/mg crea to induce sodium retention. This points to proteins that are aberrantly filtered when glomerular permeability greatly increases and resembles the definition of nephrotic syndrome in humans with a threshold of >3.5 g per day. Third, sodium retention could be completely abolished by the serine protease inhibitor aprotinin that itself is not a diuretic and does not directly block ENaC like amiloride. Fourth, volume retention was not directly related to plasma aldosterone concentration and also occurred in aldosterone-suppressed or even aldosterone-blocked conditions. This is in agreement with studies examining the role of hyperaldosteronism in experimental nephrotic syndrome in adrenalectomized rats with aldosterone-deficiency [43] and in aldosterone-resistant mice lacking the serum- and glucocorticoid kinase 1 (SGK1) by our group [22]. However, hyperaldosteronism might contribute to volume retention in experimental nephrotic model by stimulating ENaC [25, 41]. With regard to the over- and underfill hypothesis of edema formation [1, 6], this murine model contains elements of both, however, with sodium retention primarily caused by proteolytic ENaC activation and followed by underfill due to severe hypoalbuminemia. Our study shows that aprotinin emerged as a potent drug to interfere with both elements by preventing excessive proteolytic ENaC activation as well as hyperaldosteronism.

Methods

Animals

Experiments were performed on 3-month-old wild-type 129 S1/SvImJ mice purchased from Jax Mice, USA. Mice were kept on a 12:12-h light-dark cycle and fed a standard diet (ssniff, sodium content 0.24% corresponding to 104 µmol/g, Soest, Germany) with tap water ad libitum. Experimental nephrotic syndrome was induced after a single intravenous injection of doxorubicin (14.5 µg/g body weight, Cell Pharm, Bad Vilbel, Germany). Mice were kept individually in their normal cages to reduce the distress after doxorubicin injection, pellet implantation and proteinuria. Samples of spontaneously voided urine were collected in the morning 2 days before (baseline) and up to 10 days following doxorubicin injection. Daily food and fluid intake was monitored. Blood samples were drawn before induction and at sacrifice on day 10. Supplemental table 3 depicts the number of included mice and excluded/dead mice.

Treatments were performed using custom-made subcutaneous pellets with a matrix-driven sustained release (Innovative Research of America, Florida, USA). Pellets were implanted subcutaneously on the back of the mice on day 3 after doxorubicin injection. The optimal dose chosen after dose-finding studies was 1 mg per day for bovine aprotinin (6000 KIU/mg, Loxo, Heidelberg, Germany), 1.5 mg per day for camostat (kindly donated by Ono Pharmaceuticals, Osaka, Japan), and 2 mg per day for tranexamic acid (Sigma, Germany). We did not encounter any local problems with the pellets. Amiloride was administered intraperitoneally at a dose of 10 µg/g once daily. To study the role of aldosterone in volume retention, we used a high salt intake (1% in the drinking water) to suppress aldosterone secretion and potassium canrenoate to block aldosterone action (400 mg/l in the drinking water)[44] in a subgroup of animals.

Patients

Spot urine samples were obtained from patients treated for acute nephrotic syndrome in the University Hospital Tübingen between September 2012 and April 2013 [14]. Subjects evaluated for living related kidney transplantation were included as healthy controls. All human samples were obtained after informed consent. Fluid status was assessed by bioimpedance spectroscopy measurements using the Fresenius body composition monitor (BCM). Urinary amidolytic activity was determined using the chromogenic substrate S-2302 that is a substrate of serine proteases (Haemochrom, Essen, Germany). 50 µl of urine was incubated with 2 mM S-2302 for 8 h at 37°C with or without aprotinin (0.11mg/ml). The difference in optical density at 405 nm between these two conditions reflected the aprotinin-sensitive serine protease activity.

Laboratory assays

Plasma urea and creatinine as well as urinary creatinine was measured with a colorimetric assay (Labor+Technik, Berlin, Germany), plasma electrolytes and bicarbonate were measured using an IL GEM® Premier 3000 blood gas analyzer (Instrumentation Laboratory, Kirchheim, Germany). Urinary protein concentration was quantified using the Bradford method (Bio-Rad Laboratories, München, Germany), urinary sodium concentration with flame photometry (Eppendorf EFUX 5057, Hamburg, Germany). Both urinary protein and sodium concentration were normalized to the urinary creatinine concentration. Plasma aldosterone was measured using an ELISA kit (IBL, Hamburg, Germany), plasma albumin using a fluorometric kit against mouse albumin as standard (Progen, Heidelberg, Germany). Urinary amidolytic and plasmin activity were determined by incubating 3 µl urine or purified active plasmin (Merck, Darmstadt, Germany) with the chromogenic substrate S-2251 (Haemochrom, Essen, Germany) at 37°C for 1 hour. Amidolytic activity was calculated from the change in UV absorption at 405 nm. Inhibition curves were generated with serial dilution of aprotinin, camostat, tranexamic acid

and antiplasmin (Merck, Darmstadt, Germany). Urinary and plasma plasminogen concentration were measured using an ELISA kit (Loxo, Heidelberg, Germany) that detects both plasmin and plasminogen as indicated by plasmin(ogen). Urinary and plasma aprotinin concentrations were determined using an ELISA kit (Cloud-clone corp, China).

Western blots

Expression of γ-ENaC in oocytes and mouse kidney was analyzed using Western blots. Half the kidney per mouse was sliced, and the cortex was dissected using a scalpel. Homogenization was performed using a Dounce homogenisator in 1 ml lysis buffer containing 250 mM sucrose, 10 mM triethanolamine HCl, 1.6 mM ethanolamine and 0.5 EDTA at pH 7.4 (all Sigma)[37]. During all preparation steps, aprotinin (40 µg/ml) and a protease inhibitor cocktail (final concentration 0.1 x stock; mini-complete, Roche) was present to avoid γ-ENaC cleavage *in vitro*. Homogenates were centrifuged at 300,000 g for 1 h at 4°C [45], and the resulting pellet was resuspended and boiled in Laemmli buffer at 70°C for 10 min. Subsequently, 40 µg was loaded on a 7.5%-polyacrylamide gel for electrophoresis. After transfer to nitrocellulose membranes, the blocked blots were incubated with a custom-made mouse γ-ENaC antibody overnight at 4°C in a 1:500 dilution. This antibody was raised in rabbit against the sequence NTLRLDSAFSSQLTDTQLTNEF corresponding to the amino acids 634–655 of the C-terminus of murine ENaC (Pineda, Berlin, Germany,[46, 47]). For the present study, the obtained antisera were affinity-purified as described previously[48]. Blots were scanned using a fluorescence scanner (Licor Odyssey, Lincoln, NE, USA) after incubation with a secondary fluorescent donkey anti-rabbit antibody labelled with IRDye 800CW for 1 h at 4°C in a 1:20 000 dilution. To test specificity of the obtained bands, the blots were probed with the primary antibody that was pretreated with the blocking peptide overnight or the secondary antibody only. Expression of cadherin was analyzed as a loading control using a goat pan-cadherin

antibody (sc-1499, Santa Cruz, Dallas, TX, USA) and a secondary fluorescent donkey anti-goat antibody labelled with IRDye 680RD for 1 h at room temperature in a 1:20 000 dilution. Linearity of the obtained signals was tested by loading different protein amounts (Suppl. Fig. 7A,B).

For western blotting of murine γ-ENaC heterologously expressed in *Xenopus laevis* oocytes, a biotinylation approach was used to isolate cell surface proteins as described previously[7, 11, 49]. In each group, 30 oocytes expressing murine α-, β-, and γ-ENaC (1 ng of cRNA/subunit of ENaC) were subjected to biotinylation using EZ-link sulfo-NHS-SS-Biotin (Thermo Fisher Scientific, Schwerte, Germany). Oocytes were preincubated for 30 min either in ND96 solution (96mM NaCl, 2 mM KCl, 1 mM $CaCl_2$, 1 mM $MgCl_2$, 5 mM Hepes, pH 7.5) or in ND96 solution containing 2 µg/ml chymotrypsin, 500 µg/ml aprotinin, or a combination of both. After biotinylation, oocytes were lysed and proteins were precipitated with Immunopure-immobilized Neutravidin beads (Thermo Fisher Scientific). The lysates were washed with SDS-PAGE sample buffer (Roth, Karlsruhe, Germany), boiled for 5 min at 95°C, and centrifuged for 3 min at 20,000 g before loading the supernatants on a 10% SDS-PAGE gel. For detecting γ-ENaC, the anti-mouse γ-ENaC antibody described above was used in a 1:1,000 dilution. Horseradish peroxidase-labeled secondary goat anti-rabbit antibody (sc-2054, Santa Cruz, Dallas, TX, USA) was used as a 1:50,000 dilution. Chemiluminescence signals were detected using ECL Plus (GE Healthcare).

Quantitative PCR

Transcript levels of α-, β-, and γ-ENaC were analyzed using quantitative real-time PCR with the LightCycler System (Roche Diagnostics, Mannheim, Germany). Kidney tissue from the poles was homogenized using the MagNa Lyser (Roche Diagnostics, Mannheim, Germany). Cleared cell lysate was transferred for further RNA purification (RNAeasy Mini Kit, Qiagen,

Hilden, Germany). 1 µg of total RNA was reverse-transcribed to cDNA (BD Biosciences, San Jose, CA, USA) with oligo(dT) primers according to the manufacturer's protocol. Transcript levels of the target genes α-, β-,γ-ENaC and renin and the housekeeping genes GAPDH, β-actin and ribosomal protein 13 (Rps13) were determined with the primer pairs as provided in supplemental table 4. PCR reactions were performed with 2 µl cDNA, 2.4 µl $MgCl_2$ (4 mM), 1 µl primer mix (0.5 µM), 2 µl cDNA Master SYBR Green I mix (Roche Molecular Biochemicals, Mannheim, Germany), and DEPC-treated water (Advantage RT-for-PCR Kit, Clontech Laboratories, Mountain View, CA, USA), yielding a final volume of 20 µl. Melting point analysis and gel electrophoresis revealed a single product for all target and housekeeping genes. Amplification was in the linear range as analyzed with serial dilutions of the amplicons. Crossing points of the products were determined from the maxima of the second derivative of the signal curve. Absolute copy numbers were calculated from the serial dilution of the amplicons serving as standards. In addition, expression relative to the housekeeping genes Rps13 and β-actin was calculated using the ΔC_t method [50, 51]. The housekeeping gene GAPDH showed significant variation among the groups and was thus excluded from further analysis (Suppl. Fig. 5C). Amplification efficiency as analyzed by conversion of the signal slope was nearly 100% corresponding to a doubling of the product in each cycle.

Histological analyses

γ-ENaC protein expression from kidneys of healthy, nephrotic, aprotinin- and canrenoate-treated nephrotic mice were studied 8 days after doxorubicin injection (n=2-3 each) using immunofluorescence microscopy. Paraffin embedded formalin paraformaldehyde-fixed sections (2 µm) were deparaffinized and rehydrated using standard protocols. Kidney sections were blocked for 45 min with normal goat serum diluted 1:5 in 50 mM Tris pH 7.4 supplemented with 1% (w/v) skim milk (Bio-Rad Laboratories, Munich, Germany) followed

by incubation with above mentioned primary antibody (rabbit anti-γ-ENaC, 1:50) for 1 h at 37°C and subsequent washing in Tris buffer (50 mM Tris pH 7.4 supplemented with 0.05% (v/v) Tween 20; 3 x 5 min). Afterwards, the secondary antibody (goat anti-rabbit, Alexa 488; Invitrogen, 1:200) was applied for 30 min. Specificity of the γ-ENaC staining was tested using the primary antibody treated with the blocking peptide overnight. 11β-hydroxysteroid dehydrogenase type 2 (HSD2) was probed with a commercially available sheep anti-11β HSD2 antibody (AB 1296, Chemicon) and a secondary biotinylated anti-sheep antibody with subsequent detection by Streptavidin-Alexa 568 (Vector laboratories). DAPI was used to stain nuclei (1:1,000 in distilled water for 5 min) followed by rinsing in Tris buffer (3 x 5 min). Finally, sections were covered with mowiol mounting medium (Calbiochem, La Jolla, USA) and analyzed using laser scanning confocal microscopy (LSM Zeiss 710, Zeiss, Jena, Germany). γ-ENaC staining was quantified in HSD2-positive distal tubules in 20 high-power fields at 200-fold magnification using a score ranging from 0 (no staining), score 1 (weak staining), 2 (marked staining) through 3 (strong staining). Cumulated scores were divided by the number of high-power fields to obtain the final average score value. Scoring was done in an observer-blinded fashion.

Whole-cell current measurements in murine ENaC expressing oocytes using the two-electrode voltage-clamp technique

Oocytes were collected from *Xenopus laevis* as described [11, 49]. Defolliculated stage V-VI oocytes were injected with cRNA encoding murine α-, β-, and γ-ENaC (0.05-0.2 ng of cRNA/subunit of ENaC). ENaC-mediated whole-cell currents were measured using the two-electrode voltage-clamp technique two days after cRNA injection as previously described [11, 49]. Chymotrypsin and aprotinin were added as indicated at a concentration of 2 µg/ml and 500 µg/ml, respectively. Amiloride-sensitive currents (ΔI_{ami}) were determined by subtracting the

current values recorded in the presence of amiloride (2 µM) from those recorded in the absence of amiloride.

Statistical analysis

Data are provided as arithmetic means ± SEM, with n representing the number of independent experiments, N the number of batches of oocytes. Data were tested for normality with the Kolmogorov-Smirnov-Test, D'Agostino and Pearson omnibus normality test and Shapiro-Wilk-Test. Variances were tested using the Bartlett´s test for equal variances. Accordingly, data were tested for significance with parametric or nonparametric ANOVA followed by Dunnett´s, Dunn´s, or Tukey's Multiple Comparison post test, paired or unpaired Student's t-test, or Mann-Whitney U-test where applicable using GraphPad Prism 6, GraphPad Software (San Diego, CA, www.graphpad.com). Densitometric analysis of western blots was done using Image Studio Version 3.1.4 (Licor). A p value <0.05 at two-tailed testing was considered statistically significant.

Study approval

All animal experiments were conducted according to the National Institutes of Health Guide for the Care and Use of Laboratory Animals and the German Law for the Welfare of Animals, and they were approved by local authorities (Regierungspräsidium Tübingen, M5/13). The patient study was in compliance with the Declaration of Helsinki and was approved by the local ethics committee of the University Hospital Tübingen (259/2012MPG23).

Disclosures.

None.

Acknowledgement

This study was supported by a grant from the German Research Foundation (DFG, AR 1092/2-1). We further acknowledge the expert technical assistance of Antje Raiser, Dr. Melanie Märklin, Manfred Depner and Christina Lang.

References

1. Bockenhauer D. Over- or underfill: not all nephrotic states are created equal. *Pediatric nephrology (Berlin, Germany)* 2013; **28:** 1153–1156.

2. Deschenes G, Wittner M, Stefano A*, et al.* Collecting duct is a site of sodium retention in PAN nephrosis: a rationale for amiloride therapy. *J Am Soc Nephrol* 2001; **12:** 598-601.

3. Palmer LG, Frindt G. Regulation of epithelial Na channels by aldosterone. *Kitasato Med J* 2016; **46:** 1-7.

4. Rossier BC, Stutts MJ. Activation of the epithelial sodium channel (ENaC) by serine proteases. *Annual review of physiology* 2009; **71:** 361–379.

5. Passero CJ, Hughey RP, Kleyman TR. New role for plasmin in sodium homeostasis. *Curr Opin Nephrol Hypertens* 2010; **19:** 13-19.

6. Siddall EC, Radhakrishnan J. The pathophysiology of edema formation in the nephrotic syndrome. *Kidney international* 2012; **82:** 635-642.

7. Svenningsen P, Bistrup C, Friis UG*, et al.* Plasmin in nephrotic urine activates the epithelial sodium channel. *Journal of the American Society of Nephrology : JASN* 2009; **20:** 299–310.

8. Buhl KB, Friis UG, Svenningsen P*, et al.* Urinary plasmin activates collecting duct ENaC current in preeclampsia. *Hypertension* 2012; **60:** 1346–1351.

9. Svenningsen P, Andersen H, Nielsen LH*, et al.* Urinary serine proteases and activation of ENaC in kidney--implications for physiological renal salt handling and hypertensive disorders with albuminuria. *Pflügers Archiv : European journal of physiology* 2015; **467:** 531–542.

10. Passero CJ, Mueller GM, Rondon-Berrios H*, et al.* Plasmin activates epithelial Na+ channels by cleaving the gamma subunit. *The Journal of biological chemistry* 2008; **283:** 36586–36591.

11. Haerteis S, Krappitz M, Diakov A*, et al.* Plasmin and chymotrypsin have distinct preferences for channel activating cleavage sites in the gamma subunit of the human epithelial sodium channel. *The Journal of general physiology* 2012; **140:** 375–389.

12. Andersen H, Friis UG, Hansen PB*, et al.* Diabetic nephropathy is associated with increased urine excretion of proteases plasmin, prostasin and urokinase and activation of amiloride-sensitive current in collecting duct cells. *Nephrology, dialysis, transplantation : official publication of the European Dialysis and Transplant Association - European Renal Association* 2015; **30:** 781-789.

13. Buhl KB, Oxlund CS, Friis UG*, et al.* Plasmin in urine from patients with type 2 diabetes and treatment-resistant hypertension activates ENaC in vitro. *Journal of hypertension* 2014; **32:** 1672-1677; discussion 1677.

14. Schork A, Woern M, Kalbacher H*, et al.* Association of Plasminuria with Overhydration in Patients with CKD. *Clinical journal of the American Society of Nephrology : CJASN* 2016; **11:** 761-769.

15. Raij L, Tian R, Wong JS*, et al.* Podocyte injury: the role of proteinuria, urinary plasminogen, and oxidative stress. *Am J Physiol Renal Physiol* 2016; **311:** F1308-f1317.

16. Makino H, Onbe T, Kumagai I*, et al.* A proteinase inhibitor reduces proteinuria in nephrotic syndrome. *American journal of nephrology* 1991; **11:** 164-165.

17. Onbe T, Makino H, Kumagai I*, et al.* Effect of proteinase inhibitor camostat mesilate on nephrotic syndrome with diabetic nephropathy. *The Journal of diabetic complications* 1991; **5:** 167-168.

18. Maekawa A, Kakizoe Y, Miyoshi T*, et al.* Camostat mesilate inhibits prostasin activity and reduces blood pressure and renal injury in salt-sensitive hypertension. *J Hypertens* 2009; **27:** 181-189.

19. Uchimura K, Kakizoe Y, Onoue T*, et al.* In vivo contribution of serine proteases to the proteolytic activation of gammaENaC in aldosterone-infused rats. *Am J Physiol Renal Physiol* 2012; **303:** F939-943.

20. Midgley I, Hood AJ, Proctor P*, et al.* Metabolic fate of 14C-camostat mesylate in man, rat and dog after intravenous administration. *Xenobiotica; the fate of foreign compounds in biological systems* 1994; **24:** 79-92.

21. Zheng H, Liu X, Sharma NM*, et al.* Urinary Proteolytic Activation of Renal Epithelial Na+ Channels in Chronic Heart Failure. *Hypertension* 2016; **67:** 197-205.

22. Artunc F, Nasir O, Amann K*, et al.* Serum- and glucocorticoid-inducible kinase 1 in doxorubicin-induced nephrotic syndrome. *Am J Physiol Renal Physiol* 2008; **295:** F1624-1634.

23. Bohnert BN, Daniel C, Amann K*, et al.* Impact of phosphorus restriction and vitamin D-substitution on secondary hyperparathyroidism in a proteinuric mouse model. *Kidney & blood pressure research* 2015; **40:** 153-165.

24. Beath SM, Nuttall GA, Fass DN*, et al.* Plasma aprotinin concentrations during cardiac surgery: full- versus half-dose regimens. *Anesthesia and analgesia* 2000; **91:** 257-264.

25. Kim SW, Wang W, Nielsen J*, et al.* Increased expression and apical targeting of renal ENaC subunits in puromycin aminonucleoside-induced nephrotic syndrome in rats. *Am J Physiol Renal Physiol* 2004; **286:** F922-935.

26. Haerteis S, Krueger B, Korbmacher C*, et al.* The delta-subunit of the epithelial sodium channel (ENaC) enhances channel activity and alters proteolytic ENaC activation. *J Biol Chem* 2009; **284:** 29024-29040.

27. Korbmacher C, Mansley MK, Bertog M. Activation of the Epithelial Sodium Channel (ENaC) by Aldosterone in mCCDcl1 Mouse Renal Cortical Collecting Duct Cells is Dependent on SGK1 and Can be Prevented by Inhibiting Endogenous Proteases. *The FASEB Journal* 2017; **31:** 856.855.

28. Carattino MD, Mueller GM, Palmer LG*, et al.* Prostasin interacts with the epithelial Na+ channel and facilitates cleavage of the γ-subunit by a second protease. *American journal of physiology Renal physiology* 2014; **307:** F1080-1087.

29. Patel AB, Chao J, Palmer LG. Tissue kallikrein activation of the epithelial Na channel. *American journal of physiology Renal physiology* 2012; **303:** F540-550.

30. Svenningsen P, Uhrenholt TR, Palarasah Y*, et al.* Prostasin-dependent activation of epithelial Na+ channels by low plasmin concentrations. *American journal of physiology Regulatory, integrative and comparative physiology* 2009; **297:** R1733-1741.

31. Yu JX, Chao L, Chao J. Prostasin is a novel human serine proteinase from seminal fluid. Purification, tissue distribution, and localization in prostate gland. *J Biol Chem* 1994; **269:** 18843-18848.

32. Levy Yeyati N, Fellet A, Arranz C*, et al.* Amiloride-sensitive and amiloride-insensitive kaliuresis in advanced chronic kidney disease. *Journal of nephrology* 2008; **21:** 93-98.

33. Chiu TF, Bullard MJ, Chen JC*, et al.* Rapid life-threatening hyperkalemia after addition of amiloride HCl/hydrochlorothiazide to angiotensin-converting enzyme inhibitor therapy. *Annals of emergency medicine* 1997; **30:** 612-615.

34. Whiting GF, McLaran CJ, Bochner F. Severe hyperkalaemia with Moduretic. *The Medical journal of Australia* 1979; **1:** 409.

35. Jaffey L, Martin A. Malignant hyperkalaemia after amiloride/hydrochlorothiazide treatment. *Lancet (London, England)* 1981; **1:** 1272.

36. Mangano DT, Tudor IC, Dietzel C. The risk associated with aprotinin in cardiac surgery. *The New England journal of medicine* 2006; **354:** 353-365.

37. Yang L, Frindt G, Lang F*, et al.* SGK1-dependent ENaC processing and trafficking in mice with high dietary K intake and elevated aldosterone. *Am J Physiol Renal Physiol* 2016**:** ajprenal.00257.02016.

38. Kleyman TR, Carattino MD, Hughey RP. ENaC at the cutting edge: regulation of epithelial sodium channels by proteases. *The Journal of biological chemistry* 2009; **284:** 20447–20451.

39. Frindt G, Ergonul Z, Palmer LG. Surface expression of epithelial Na channel protein in rat kidney. *J Gen Physiol* 2008; **131:** 617-627.

40. Patel AB, Frindt G, Palmer LG. Feedback inhibition of ENaC during acute sodium loading in vivo. *Am J Physiol Renal Physiol* 2013; **304:** F222-232.

41. de Seigneux S, Kim SW, Hemmingsen SC*, et al.* Increased expression but not targeting of ENaC in adrenalectomized rats with PAN-induced nephrotic syndrome. *Am J Physiol Renal Physiol* 2006; **291:** F208-217.

42. Jacquillet G, Chichger H, Unwin RJ*, et al.* Protease stimulation of renal sodium reabsorption in vivo by activation of the collecting duct epithelial sodium channel (ENaC). *Nephrology, dialysis, transplantation : official publication of the European Dialysis and Transplant Association - European Renal Association* 2013; **28:** 839–845.

43. Lourdel S, Loffing J, Favre G*, et al.* Hyperaldosteronemia and activation of the epithelial sodium channel are not required for sodium retention in puromycin-induced nephrosis. *J Am Soc Nephrol* 2005; **16:** 3642-3650.

44. Artunc F, Ebrahim A, Siraskar B*, et al.* Responses to diuretic treatment in gene-targeted mice lacking serum- and glucocorticoid-inducible kinase 1. *Kidney & blood pressure research* 2009; **32:** 119-127.

45. Picard N, Eladari D, El Moghrabi S*, et al.* Defective ENaC processing and function in tissue kallikrein-deficient mice. *J Biol Chem* 2008; **283:** 4602-4611.

46. Nesterov V, Krueger B, Bertog M*, et al.* In Liddle Syndrome, Epithelial Sodium Channel Is Hyperactive Mainly in the Early Part of the Aldosterone-Sensitive Distal Nephron. *Hypertension (Dallas, Tex : 1979)* 2016; **67:** 1256-1262.

47. Krueger B, Haerteis S, Yang L*, et al.* Cholesterol depletion of the plasma membrane prevents activation of the epithelial sodium channel (ENaC) by SGK1. *Cell Physiol Biochem* 2009; **24:** 605-618.

48. Vallur R, Kalbacher H, Feil R. Catalytic activity of cGMP-dependent protein kinase type I in intact cells is independent of N-terminal autophosphorylation. *PloS one* 2014; **9:** e98946.

49. Haerteis S, Krappitz A, Krappitz M*, et al.* Proteolytic activation of the human epithelial sodium channel by trypsin IV and trypsin I involves distinct cleavage sites. *The Journal of biological chemistry* 2014; **289:** 19067–19078.

50. Livak KJ, Schmittgen TD. Analysis of relative gene expression data using real-time quantitative PCR and the 2(-Delta Delta C(T)) Method. *Methods (San Diego, Calif)* 2001; **25:** 402-408.

51. Wagner CA, Loffing-Cueni D, Yan Q*, et al.* Mouse model of type II Bartter's syndrome. II. Altered expression of renal sodium- and water-transporting proteins. *Am J Physiol Renal Physiol* 2008; **294:** F1373-1380.

Figure 1. Characteristics of experimental nephrotic syndrome in 129S1/SvImJ mice.
Following a single doxorubicin dose all hallmarks of human nephrotic syndrome were present including proteinuria and hypoalbuminemia (A), body weight gain and urinary sodium retention (B). Proteinuria was paralleled by urinary amidolytic activity against S-2251 and urinary plasmin(ogen) excretion leading to decrease of plasma plasminogen concentration (C). Inhibition curves for amidolytic activity in nephrotic urine (D). Pooled curve from n=5-7 single curves with final concentration of urinary protein between 4000 - 6000 µg/ml.
Arithmetic means ± SEM. # indicates significant difference to baseline value.

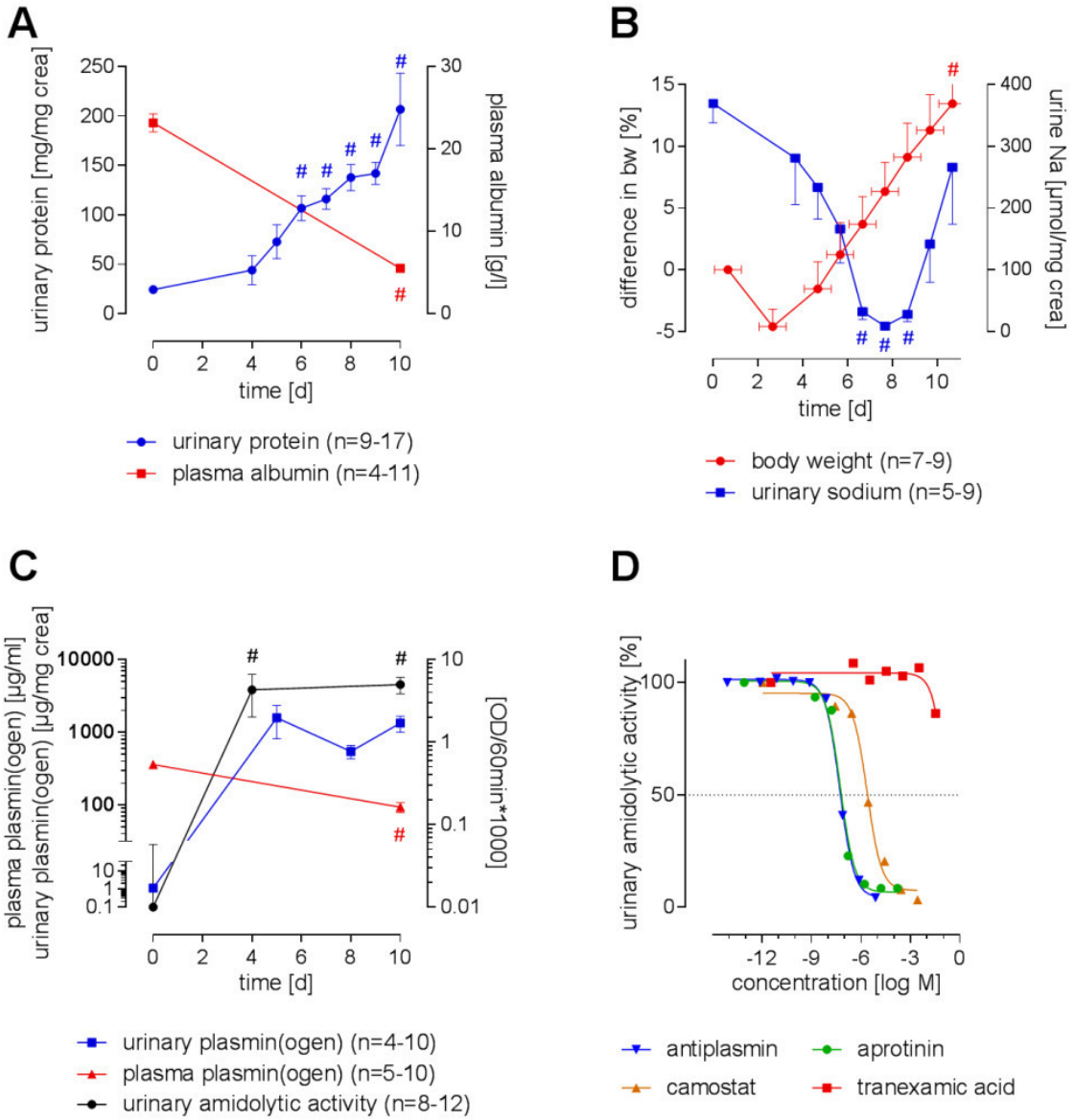

Figure 2: Aprotinin-sensitive proteasuria and overhydration in nephrotic patients
Urine samples from patients with nephrotic syndrome exhibit high proteinuria (A) and urinary serine protease activity that is sensitive to aprotinin (B). This is paralleled by massive overhydration as assessed with bioimpendance spectroscopy (C).
§ indicates significant difference between healthy subjects and nephrotic patients. OD optical density at 405 nm

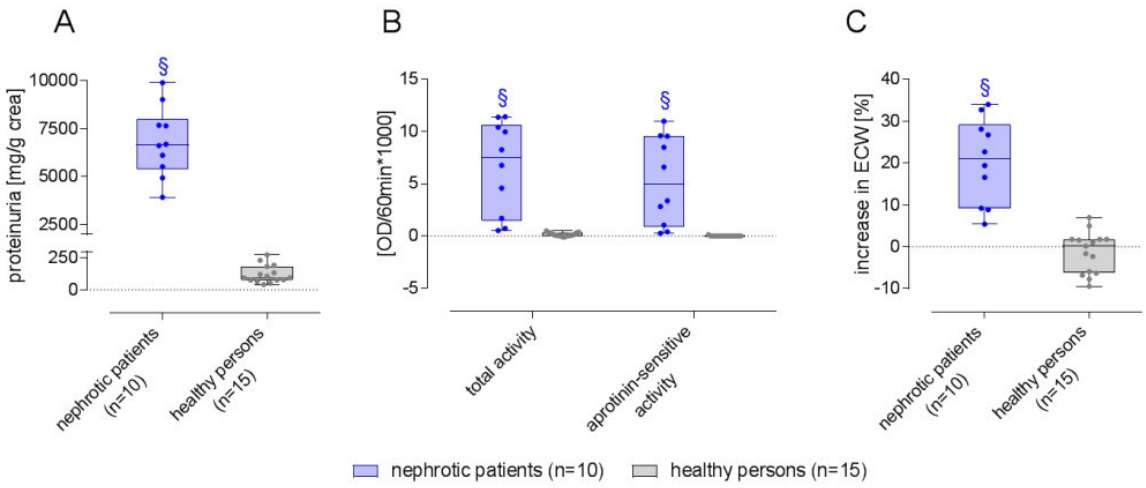

Figure 3. Treatment of nephrotic mice with aprotinin, camostat and tranexamic acid.
Course of proteinuria (A; inset: maxima), urinary amidolytic activity (B, inset: maxima), body weight (C; inset: maxima) and urinary sodium/creatinine ratio (D; inset: minima) in nephrotic mice treated with placebo, aprotinin, camostat or tranexamic acid. Urinary and plasma aprotinin concentration during treatment with 1 mg/d aprotinin (E) and dose-response curves showing the relationship between urinary aprotinin concentration and inhibition of amidolytic activity (*in vitro* and *in vivo*, resp.) and maximal body weight gain (F).
Arithmetic means ± SEM. # indicates significant difference to baseline value, * indicates significant difference between aprotinin and placebo-treated mice.

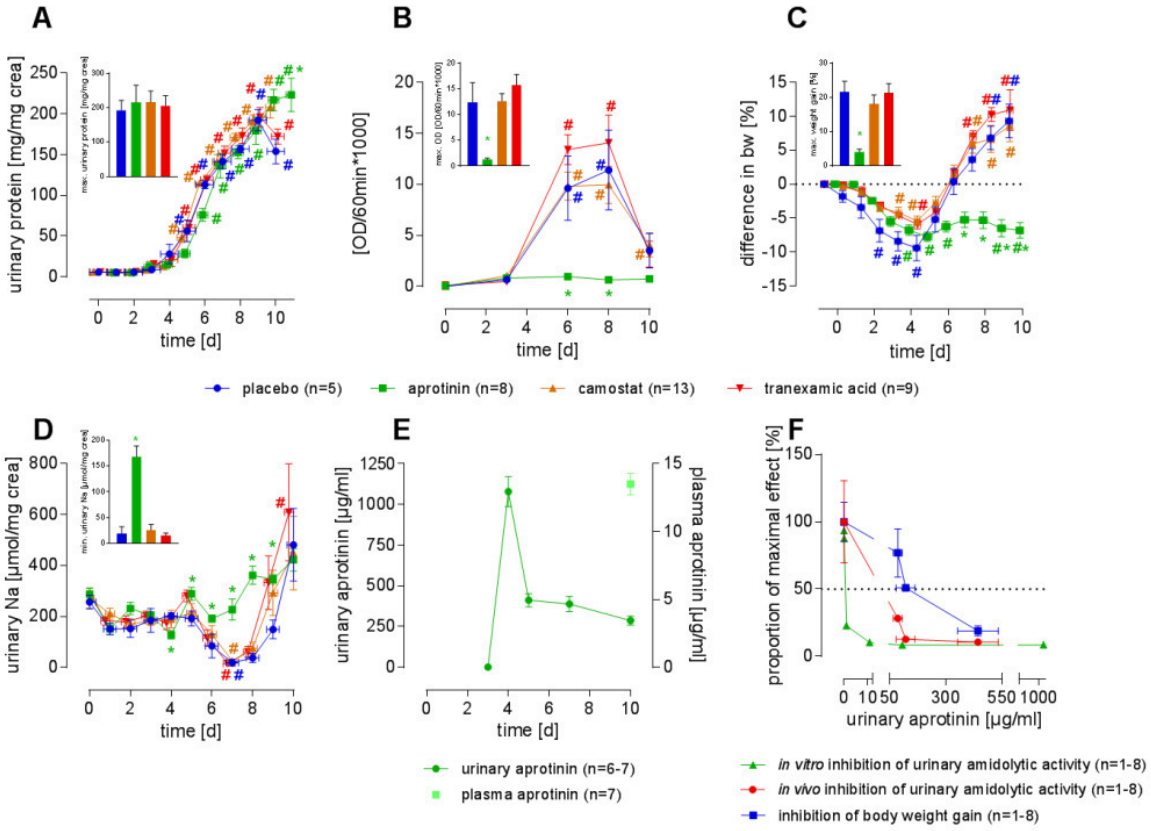

Figure 4. Effect of amiloride and canrenoate treatment in nephrotic mice and role of plasma aldosterone

Course of proteinuria (A; inset: maxima), body weight (B; inset: maxima) and urinary Na excretion (C; inset: minima) in nephrotic mice treated with vehicle, amiloride (10 µg/g i.p.) or canrenoate (400 mg/l in the drink, intake on average 95 µg/g). Urine was collected 4 hours after injection of vehicle or amiloride. Plasma aldosterone concentration during treatment with serine protease inhibitors (D, apr=aprotinin, cam=camostat, txa=tranexamic acid) as well as transcript levels of renin (E) in healthy, placebo and aprotinin-treated nephrotic mice normalized to the housekeeping gene Rps13 in healthy, placebo and aprotinin-treated nephrotic mice (n=8-9 each).

Arithmetic means ± SEM. # indicates significant difference to baseline value (A-C) or healthy (D-E), * indicates significant difference between placebo and amiloride-treated nephrotic mice (A-C) or between placebo and aprotinin-treated nephrotic mice (E).

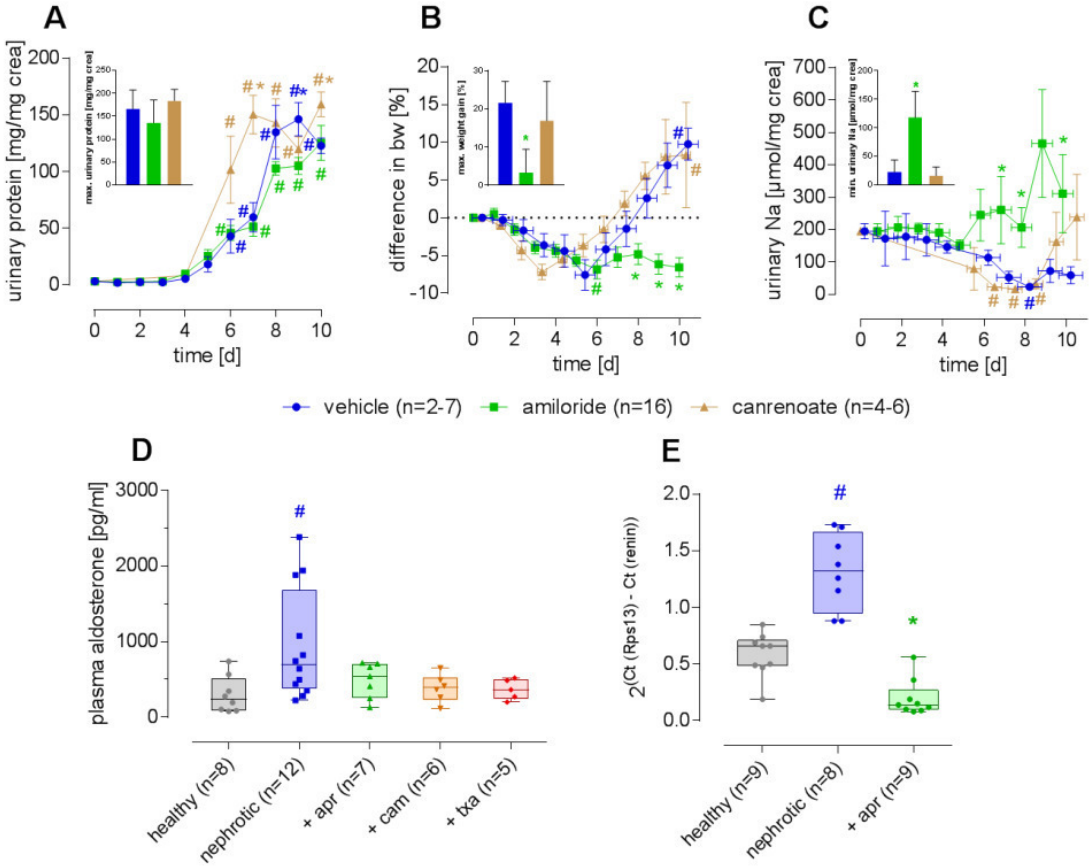

Figure 5. Expression of γ-ENaC in renal cortex

(A) Relative mRNA expression of the α-, β- and γ-subunit of ENaC in healthy, placebo-treated nephrotic and aprotinin-treated nephrotic mice normalized to the housekeeping gene Rps13 that had constant expression across the groups (n=8-9 each).

(B) Western blot from renal cortex showing several bands between 44 and 86 kDa. Administration of the blocking peptide attenuated bands at 44, 53, 70, 76 and 86 kDa while bands at 65 and 48 kDa were not blocked.

(C) γ-ENaC contains two cleavage sites within the pore-forming loop for post-translational proteolytic processing. At amino acid (aa) position 143, γ-ENaC is cleaved intracellularly by the serine protease furin, at aa 186 extracellularly in the tubulus lumen by an extracellular serine protease. The molecular weights of full-length and furin-cleaved γ-ENaC are 15 kDa apart, those between furin and extracellularly cleaved γ-ENaC 5 kDaas detected by an antibody against the C terminus of γ–ENaC.

(D) Western blots from membrane proteins of healthy, placebo-treated nephrotic and aprotinin-treated nephrotic mice. Cadherin expression at 125 kDa served as a loading control.

(E) Relative abundance of the 44, 53, 70, 76 and 86 kDa bands in healthy, placebo-treated nephrotic and aprotinin-treated nephrotic mice normalized to the cadherin expression.

# indicates significant difference to healthy mice, * indicates significant difference between placebo and aprotinin-treated nephrotic mice.

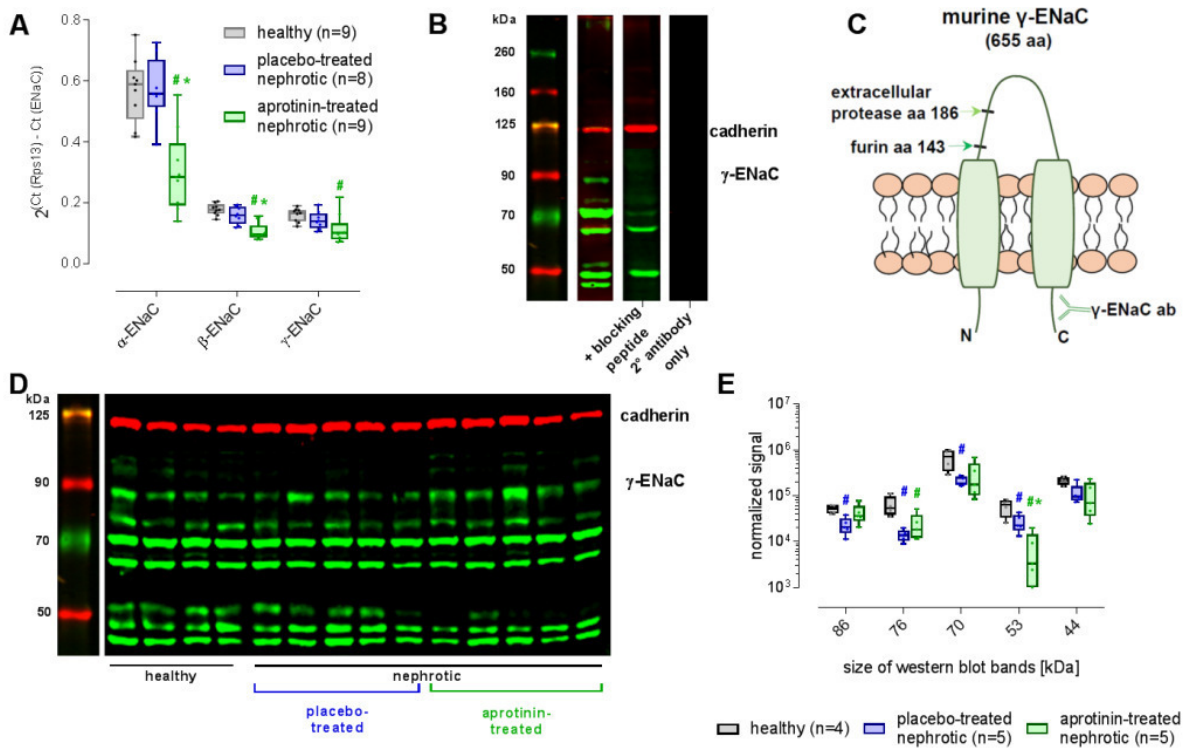

Figure 6. Histological expression of γ-ENaC in the aldosterone-sensitive distal nephron
Immunofluorescence of fixed kidney sections from healthy and nephrotic mice treated with placebo or aprotinin at 200-fold magnification (scale=50 µm). Inset: 630-fold magnification corresponding to 28 x 28 µm. Antibodies are directed against γ-ENaC (green) and 11β-hydroxysteroid dehydrogenase type 2 (red) defining the distal nephron. Nuclei are stained blue with DAPI.

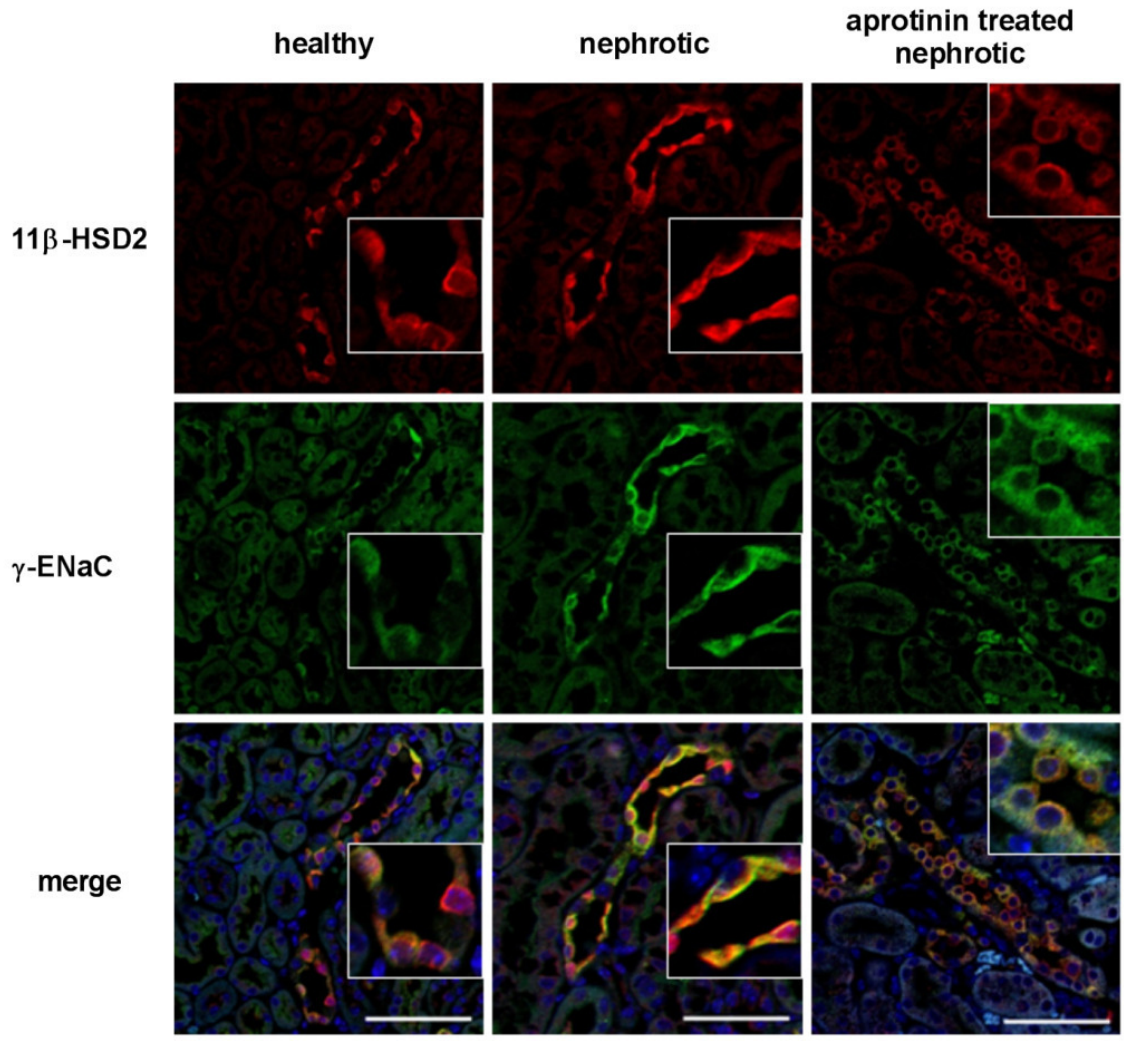

Figure 7. Aprotinin has no inhibitory effect on ENaC activity and prevents the appearance of a γ-ENaC cleavage product at 67 kDa

(A-B) Representative whole-cell current traces from oocytes expressing murine ENaC. Amiloride (ami, 2 µM) or aprotinin (aprot, 500 µg/ml) were present in the bath solution as indicated.

(C) Summary of similar experiments as shown in A or B. Data points obtained from individual oocytes are connected by a line.

(D) Expression of biotinylated γ–ENaC at the cell surface analyzed by SDS-PAGE. Oocytes expressing murine ENaC were preincubated for 30 min in protease-free control solution (co) or in solution containing chymotrypsin (chy), chymotrypsin+aprotinin (chy+aprot) or aprotinin (aprot). γ–ENaC was detected with an antibody against the C terminus of murine γENaC. This antibody detected an unspecific band of ~130 kDa that was also present in non-injected (n.i.) oocytes.

N indicates the number of different batches of oocytes.

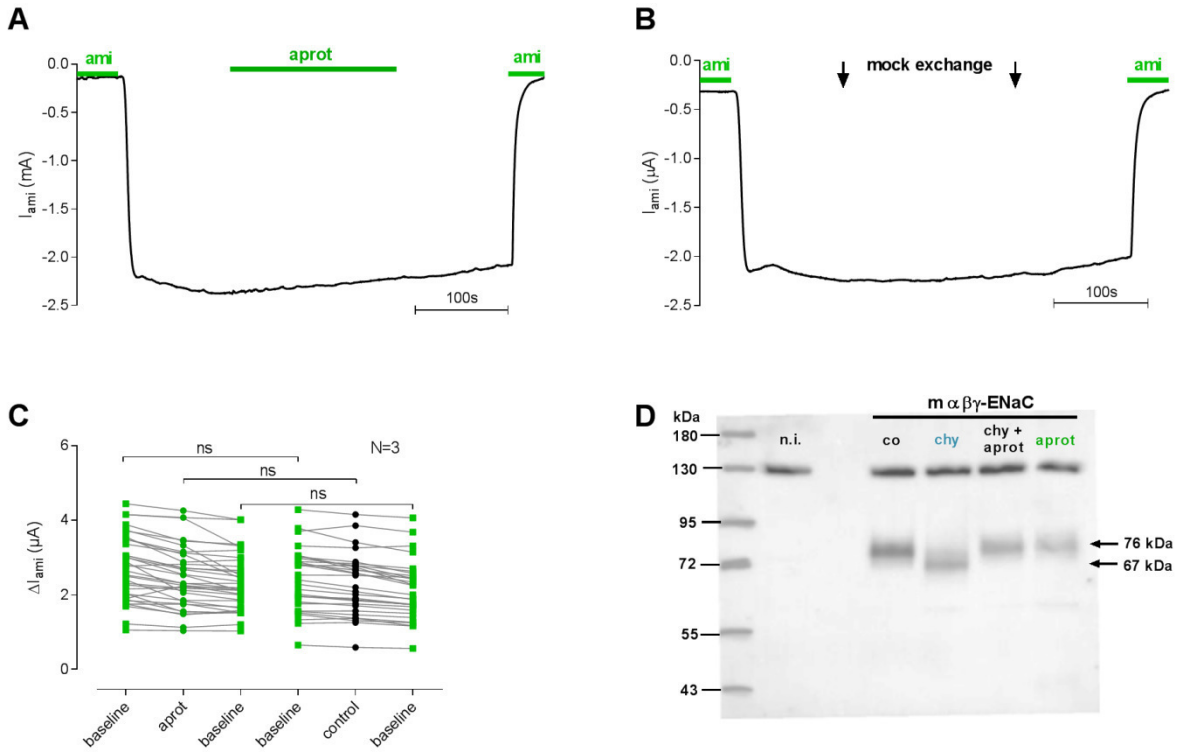

Table 1. Plasma values after 10 days of treatment with aprotinin, camostat and tranexamic acid in nephrotic mice.

Arithmetic means of n=4-12 mice per group ± SEM. # indicates significant difference to healthy mice.

parameter	healthy mice	nephrotic mice treated with			
		placebo	aprotinin	camostat	tranexamic acid
plasma Na, mM	152±1	145±1 #	148±1	145±1 #	145±1 #
plasma K, mM	4.3±0.1	4.7±0.1	5.0±0.2	4.9±0.1#	5.0±0.1 #
plasma bicarbonate, mM	22±1	27±1	28±1 #	28±1 #	28±1 #
venous pH	7.31±0.01	7.36±0.01 #	7.37±0.01 #	7.37±0.01 #	7.36±0.01 #
plasma urea, mg/dl	34±2	35±12	63±16	52±13	31±5
plasma creatinine, mg/dl	0.24±0.03	0.61±0.14	0.44±0.12	0.49±0.09	0.74±0.19 #
plasma albumin, g/l	20.3±0.2	6.7±0.3 #	7.5±0.7 #	7.0±0.6 #	6.8±0.4 #

Suppl. Fig. 1. Characteristics of experimental nephrotic syndrome in 129S1/SvImJ mice (continued).
Nephrotic mice developed ascites (A, upper mouse) and visible lipemia (B, right capillary). Note also reduced hematocrit as correlate of volume retention. Although food and fluid intake remained fairly constant (C) there is a marked renal sodium avidity indicated by a fall in the urinary Na/K ratio (D).
Arithmetic means ± SEM. # indicates significant difference to baseline value.

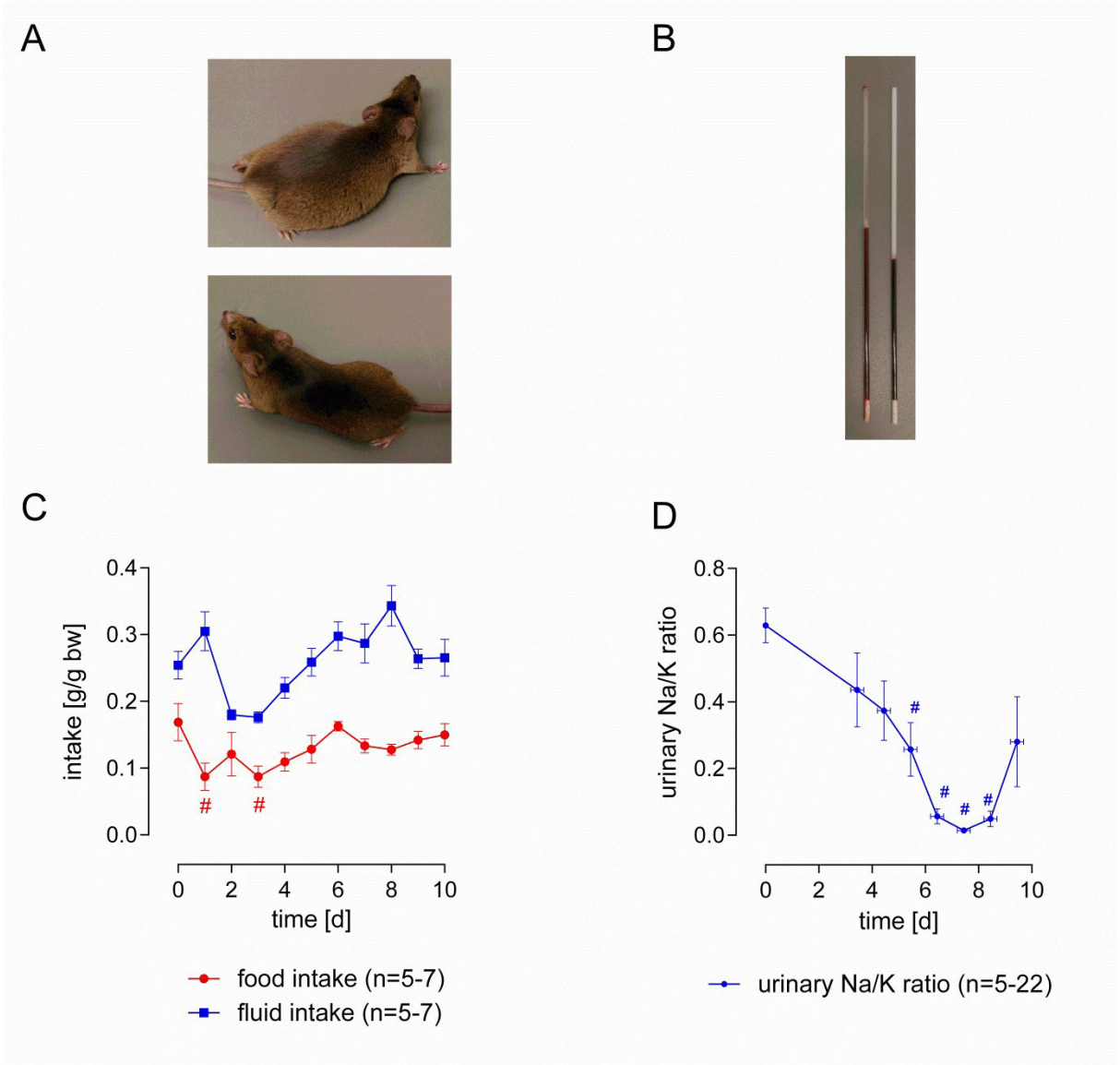

Suppl. Fig 2. Inhibition curves for amidolytic activity with purified active plasmin.
Pooled curve from n=5-7 single curves using a final concentration plasmin concentration in the well of 27 µg/ml.

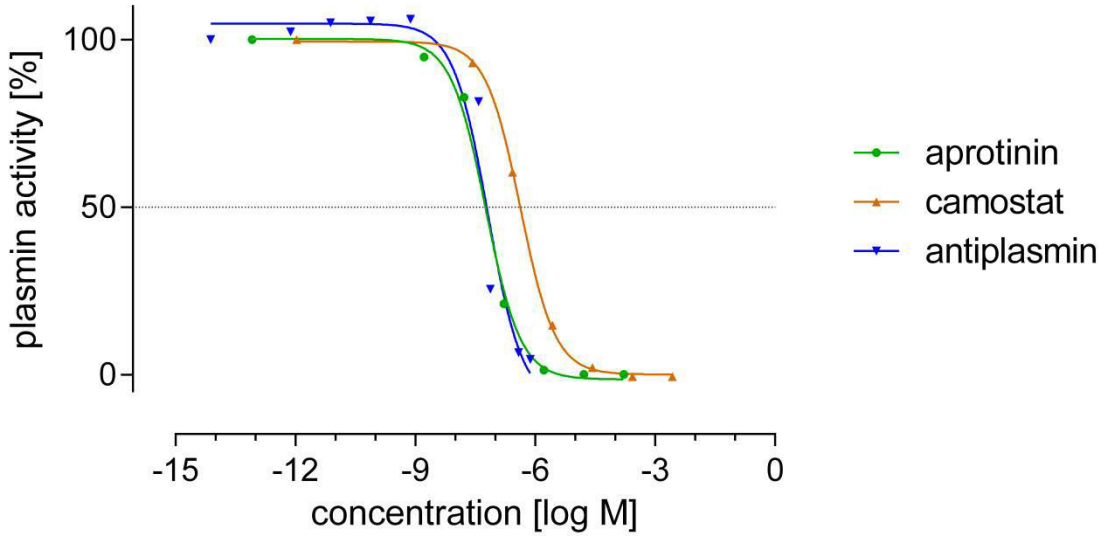

Suppl. table 1: Calculated IC_{50} values and comparison between urinary amidolytic and plasmin activity.

inhibitor	urinary amidolytic activity	plasmin activity	p
aprotinin	72 ± 32 nM (0.5 ± 0.2 µg/ml)	58 ± 12 nM (0.4 ±0.1 µg/ml)	0.5582
camostat	2344 ± 676 nM (1.2 ± 4.4 µg/ml)	427 ± 20 nM (0.2 ± 0.1 µg/ml)	0.0003
anti-plasmin	51 ± 5 nM (3.6 ± 0.03 µg/ml)	66 ± 34 nM (4.6 ± 0.2 µg/ml)	0.5967

Suppl. table 2: Patient characteristics, fluid status and urinary amidolytic activity. Medians with interquartile range.

	healthy (n=15)	**patients with acute nephrotic syndrome (n=10)**	**p**
median age, years	50 (42; 62)	53 (41; 69)	0.5883
gender distribution	73% ♀ / 27% ♂	40% ♀ / 60% ♂	0.0694
estimated GFR, ml/min/1.73 m²	97 (77; 112)	35 (20; 69)	<0.0001
proteinuria, mg/g crea	95 (77; 185)	6660 (5379; 8023)	<0.0001
diagnoses	n.a.	membranous GN (30%), IgA-GN (30%), thrombotic microangiopathy (10%), membranoproliferative GN (10%), microscopic polyangiitis (10%), unknown (10%)	
extracellular water (ECW), l/1.73 m²	14.8 (14.1; 15.5)	18.0 (16.6; 19.4)	<0.0001
intracellular water (ICW), l/1.73 m²	17.4 (16.6; 18.8)	18.3 (16.3; 19.8)	0.6080
overhydration (OH), l/1.73 m²	0 (-0.9; +0.2)	+3.8 (+1.5; +5.7)	0.0001
ECW/ICW	0.85 (0.80; 0.88)	1.03 (0.91; 1.12)	0.0007
total urinary amidolytic activity, OD/60 min	0.004 (0.002; 0.018)	0.341 (0.058; 0.572)	0.0001
urinary aprotinin-sensitive amidolytic activity, OD/60 min	0.0003 (0.0003; 0.0003)	0.299 (0.089; 0.558)	<0.0001
urinary aprotinin-sensitive amidolytic activity, % of total activity	5 (2; 10)	79 (58; 94)	<0.0001

Abbreviations: n.a., not applicable; GN, glomerulonephritis; ECW extracellular water; ICW, intracellular water; OH, overhydration; OD optical density

Suppl. Fig. 3. Food and fluid intake (A-B) as well as renal sodium avidity indicated by the urinary Na/K ratio (C) during treatment with pellets containing placebo, aprotinin, camostat and tranexamic acid.

Arithmetic means ± SEM. # indicates significant difference to baseline value, * indicates significant difference between placebo and aprotinin-treated mice.

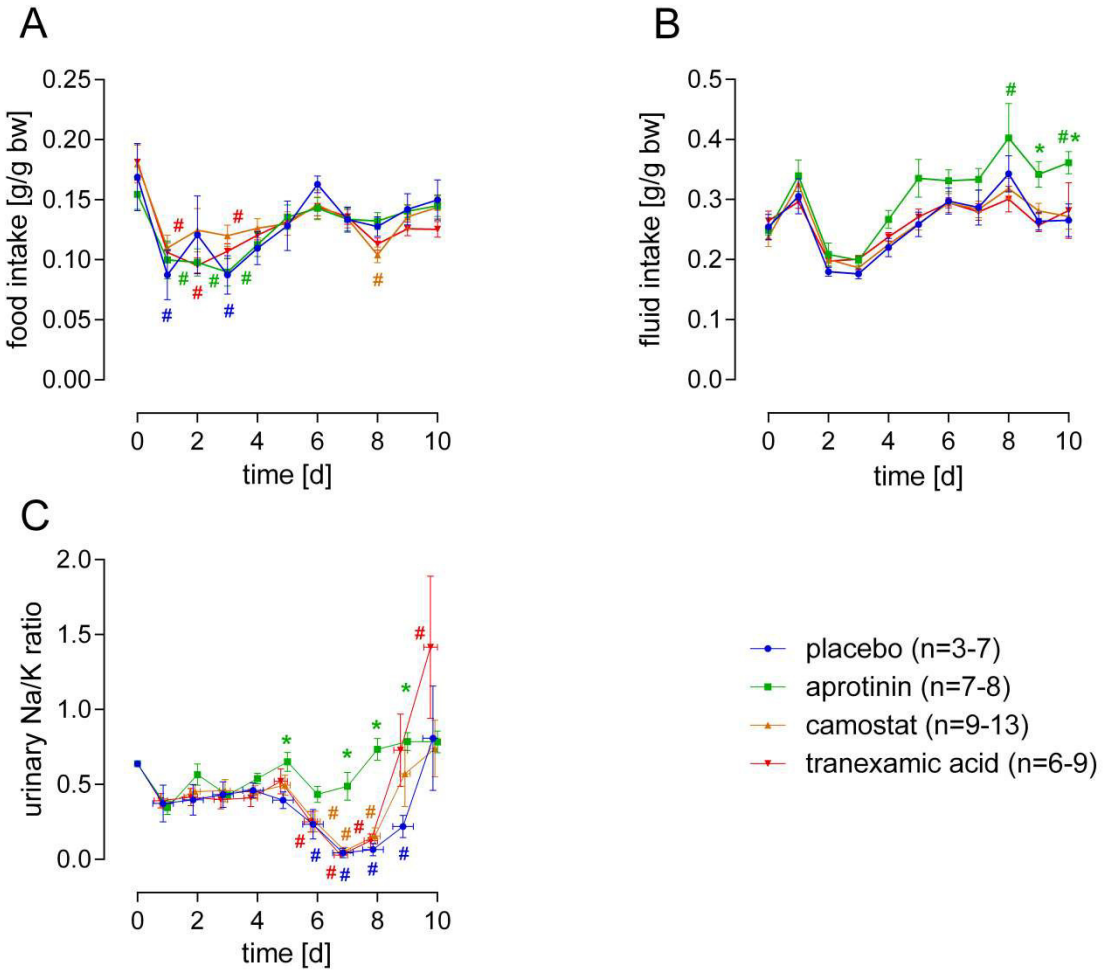

Suppl. Fig. 4. Effect of high salt intake on aldosterone secretion and volume retention in healthy and nephrotic mice.

(A) In healthy mice, body weight remained stable under high salt (hs) intake with 1% NaCl in the drinking water while aldosterone secretion was significantly suppressed. After injection of doxorubicin and onset of proteinuria nephrotic mice treated with placebo pellets developed marked volume retention, and plasma aldosterone concentration remained suppressed. Aprotinin treatment prevented body weight gain completely. This longitudinal experiment indicates that proteinuria confers salt sensitivity to formerly salt-insensitive mice, which is independent from aldosterone and relates to urinary excretion of aprotinin-sensitive serine proteases.

(B) Plasma aldosterone concentration at the day 10 after doxorubicin injection and maximal body weight gain during various treatments (apr=aprotinin, amil=amiloride, can=canrenoate, cam=camostat, txa=tranexamic acid, hs=high salt, plac=placebo). Note the different pattern of both parameters.

Arithmetic means ± SEM. # indicates significant difference to baseline value, * indicates significant difference between placebo and aprotinin-treated mice.

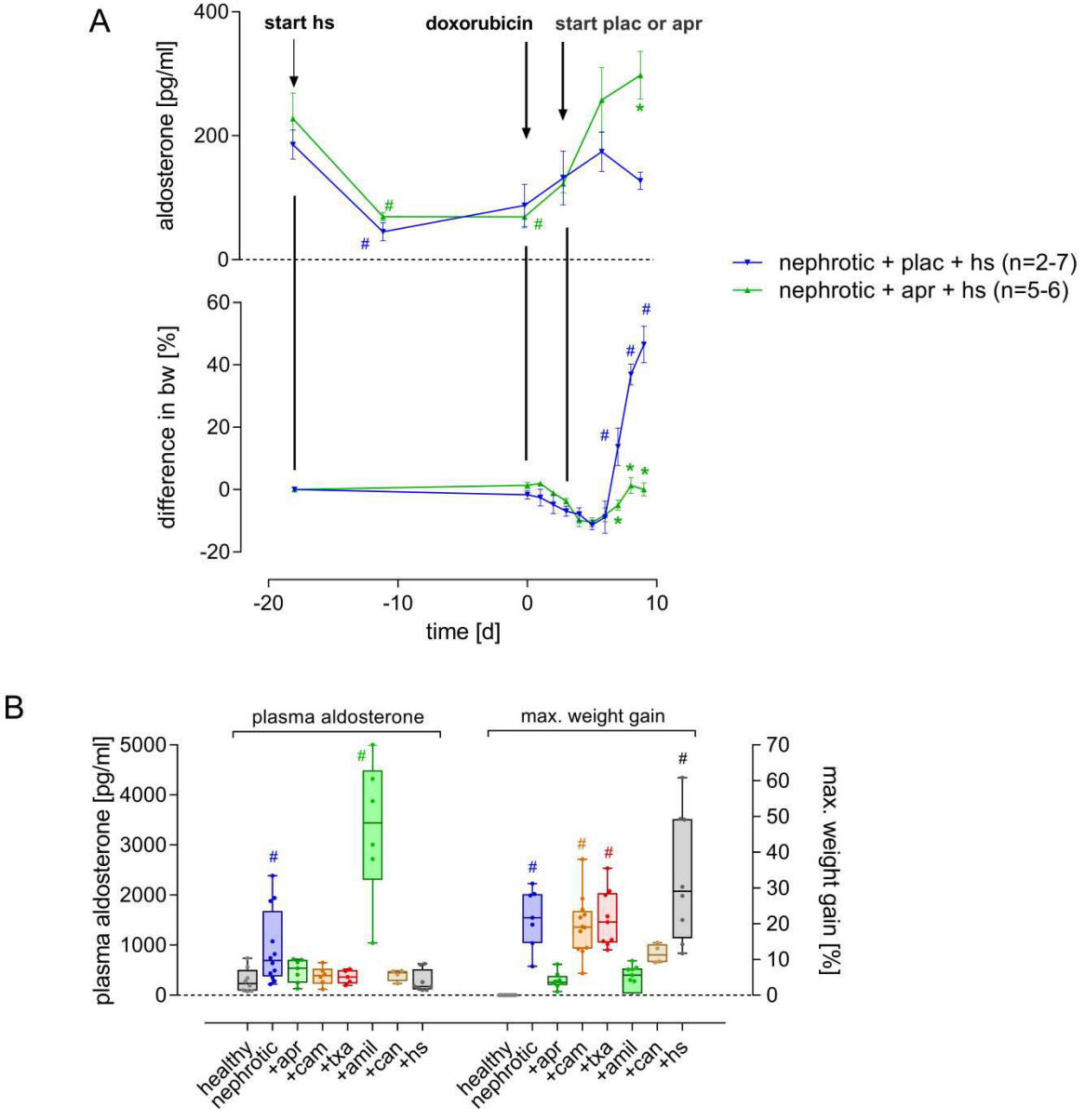

Suppl. Fig. 5: mRNA Expression of renin and the housekeeping genes in healthy and nephrotic mice

(A) Absolute mRNA expression of renin in healthy, placebo and aprotinin-treated nephrotic mice (n=8-9 each).

(B) Relative mRNA expression of renin normalized to the housekeeping gene β-actin in healthy, placebo and aprotinin-treated nephrotic mice (n=8-9 each).

(C) Absolute mRNA expression of the housekeeping genes GAPDH, Rps13 and β-actin in healthy, placebo-treated nephrotic and aprotinin-treated nephrotic mice (n=8-9 each). Note that the GAPDH expression is significantly decreased in aprotinin-treated nephrotic mice.

Arithmetic means ± SEM. # indicates significant difference to baseline value, * indicates significant difference between placebo and aprotinin-treated mice.

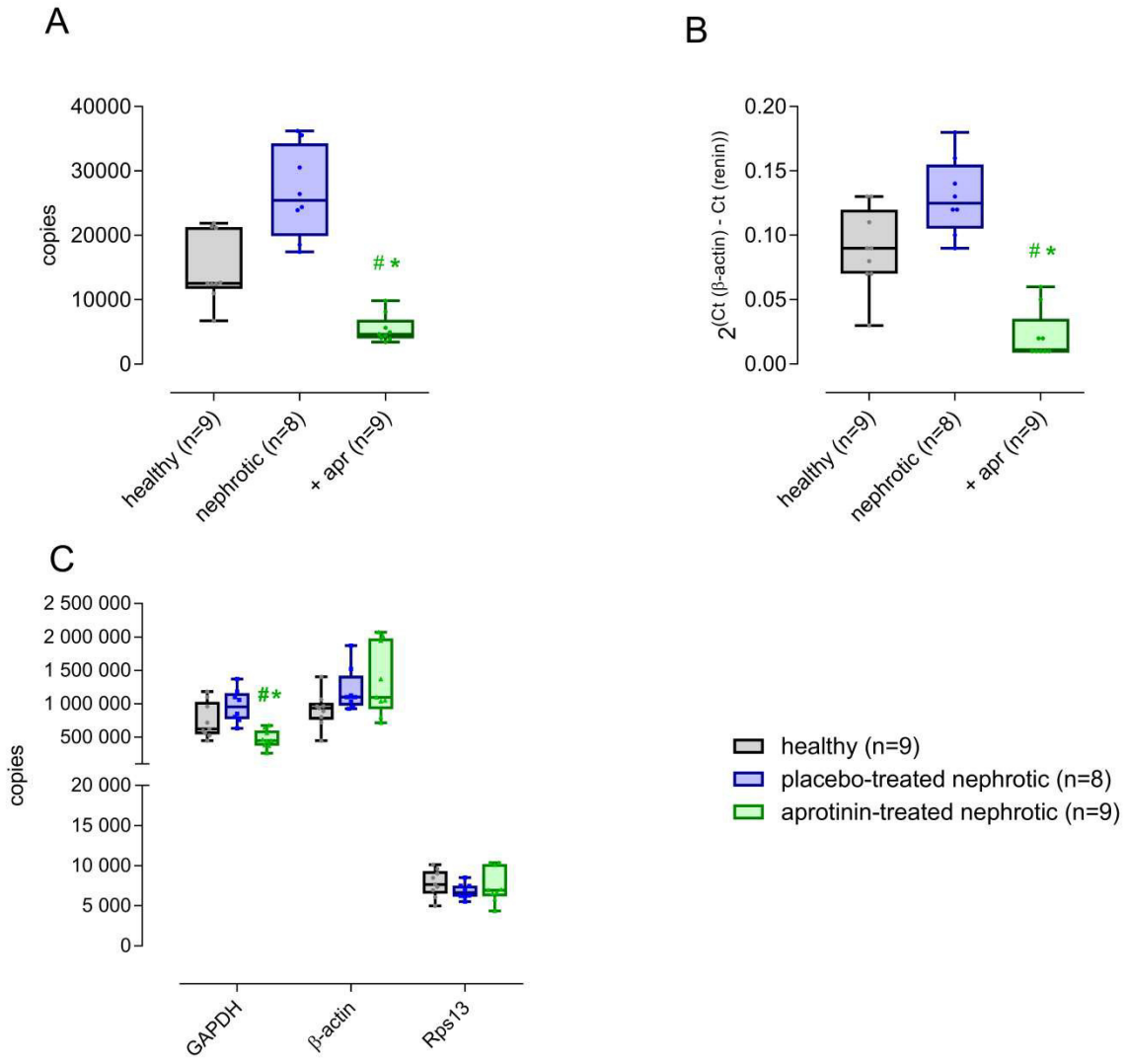

Suppl. Fig. 6: Expression of ENaC subunits in healthy and nephrotic mice

(A) Absolute mRNA expression of the α-, β- and γ-subunit of ENaC in healthy, placebo-treated nephrotic and aprotinin-treated nephrotic mice (n=8-9 each).

(B) Relative mRNA expression of the α-, β- and γ-subunit of ENaC normalized to the housekeeping gene β-actin in healthy, placebo-treated nephrotic and aprotinin-treated nephrotic mice (n=8-9 each).

# indicates significant difference to healthy mice, * indicates significant difference between placebo and aprotinin-treated nephrotic mice.

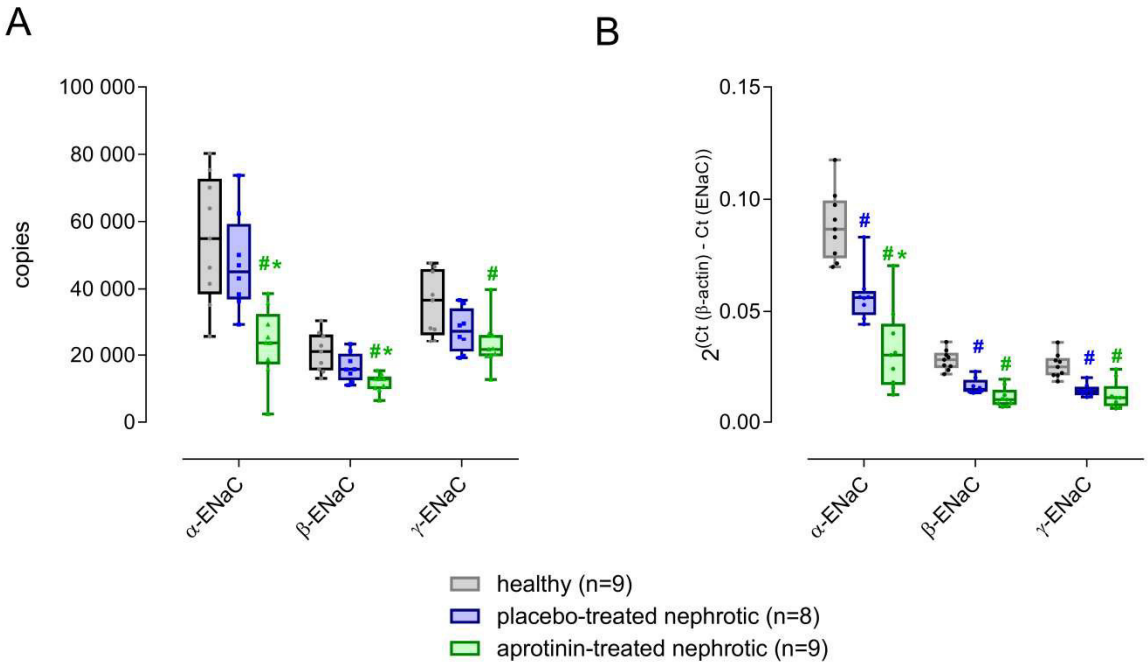

Suppl Fig. 7: Expression of γ-ENaC in renal cortex analysed by Western blot
(A-B) Western blot from renal cortex demonstrating linearity of the signal obtained for the expression of the loading control cadherin and the γ-ENaC bands at 53, 70 and 86 kDa.

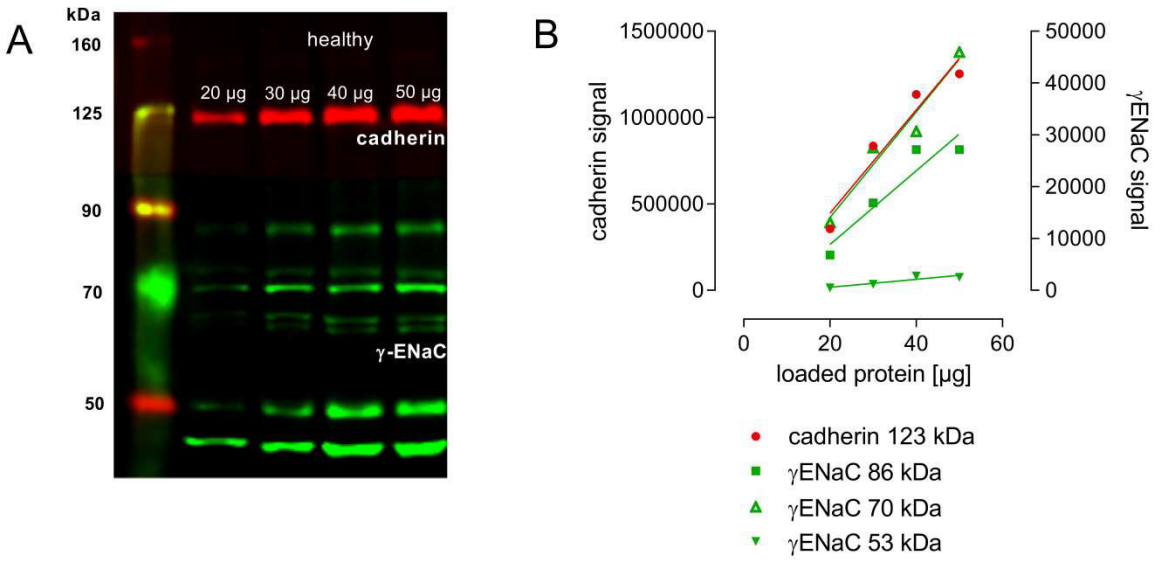

Suppl. Fig. 8: Semiquantitative analysis and specificity of γ-ENaC staining in the aldosterone-sensitive distal nephron

(A) Cross-sections at 200-fold magnification were analysed using a staining score [0=no, 1=weak, 2=marked, 3=strong staining] in healthy and nephrotic mice treated with placebo, aprotinin (apr) (n=2-3 each, N= total number of analysed high power fields).

(B) Immunofluoresence using the primary γ-ENaC antibody in the presence of the blocking peptide.

# indicates significant difference to healthy mice, * indicates significant difference between placebo and aprotinin-treated nephrotic mice.

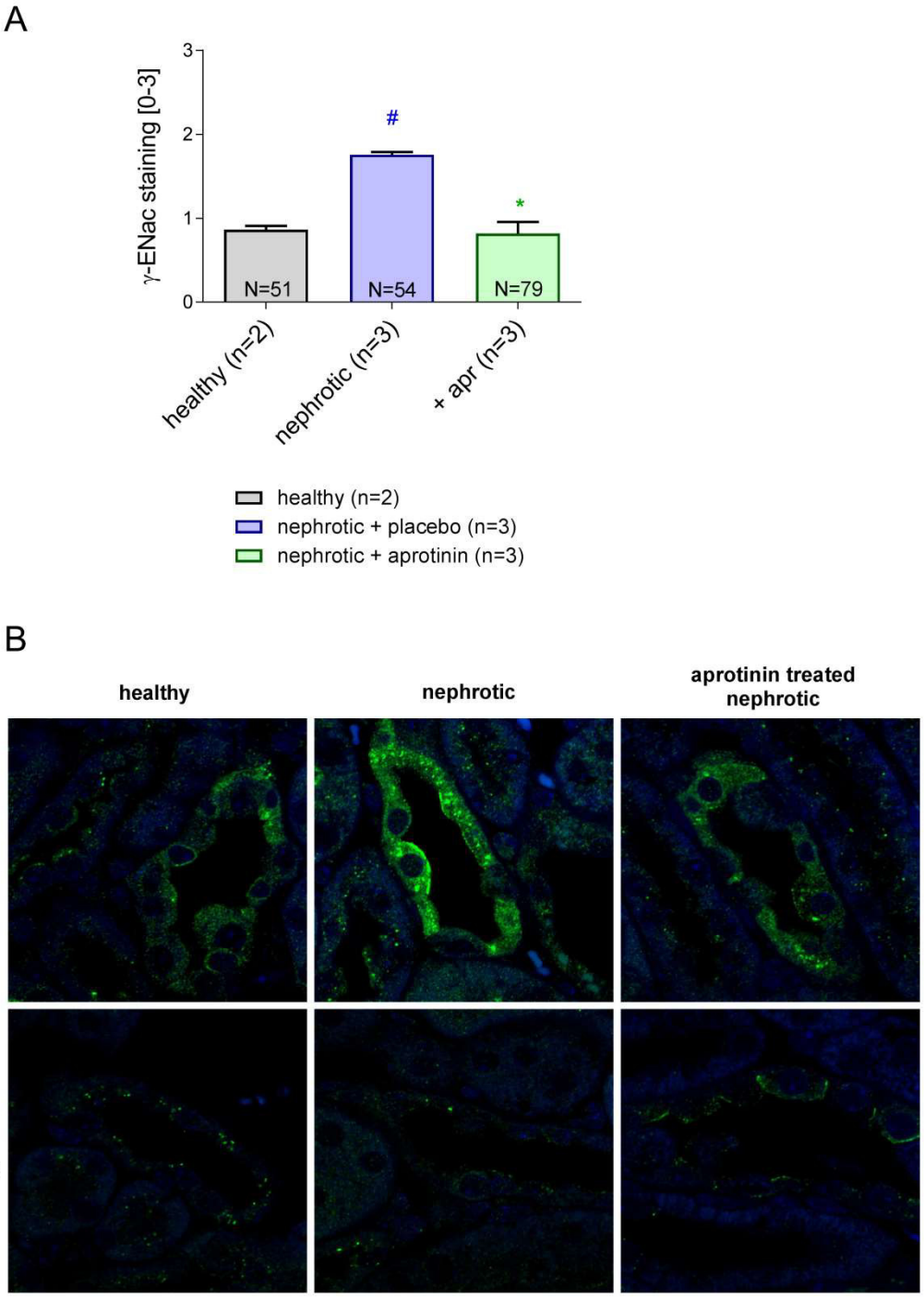

Suppl. Fig. 9. Aprotinin prevents proteolytic activation of ENaC by chymotrypsin and pre-incubation with aprotinin has no effect on baseline ΔI_{ami}

(A-C) (upper figure) Representative whole-cell current traces from oocytes expressing murine ENaC. Amiloride (ami, 2 µM), chymotrypsin (chy, 2 µg/ml) -/+ aprotinin (aprot, 500 µg/ml) (chy+aprot) were present in the bath solution as indicated.

(lower figure) Summary of similar experiments as shown in the representative traces. Data points obtained from individual oocytes are connected by a line.

(D) Oocytes expressing murine ENaC were preincubated for 48 h with or without aprotinin (500 µg/ml). To pool data from different batches of oocytes, individual ΔI_{ami} values were normalized to the mean ΔI_{ami} value of the control group (- chy).

N indicates the number of different batches of oocytes. # indicates significant differences between indicated groups.

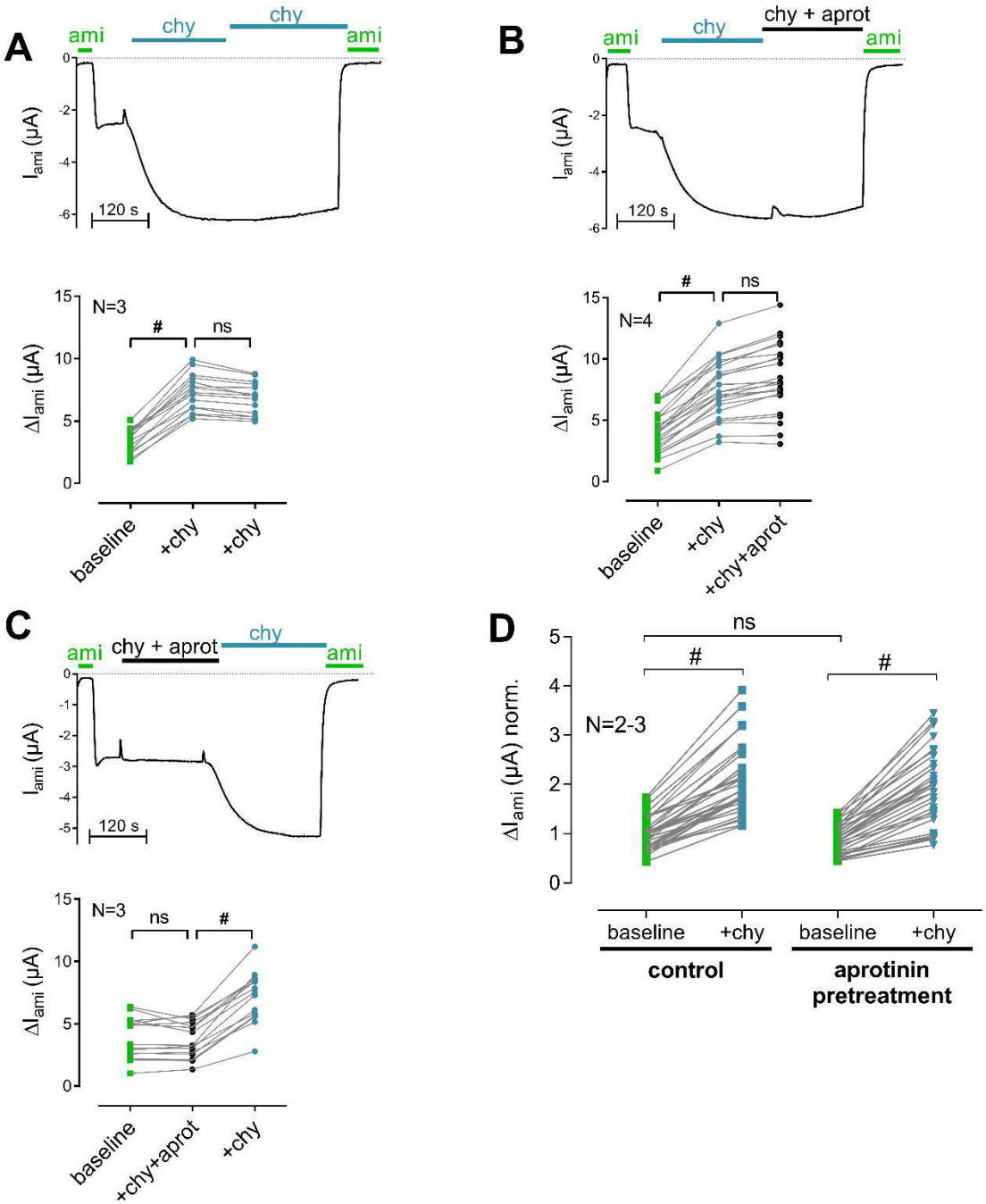

Supplemental table 3. Number of included and excluded mice.

mice	Σ [mice]	[%]
total	128	100
included	104	81
excluded all	24	19
excluded due to lack of response (non-nephrotic proteinuria <140 mg/mg creatinine after 7 days)	19	15
excluded due to toxicity within 7 days (plasma urea > 140 mg/dl, orbital paravasate and necrosis or death)	5	4

Supplemental table 4. Used primers.

gene	sense/forward 5'→3' orientation	antisense/reverse 5'→3' orientation	amplicon	reference
α-ENaC	GGTGCACGGTCAGGATGAG	TAGTTGCCTCCGAGGCTGTC	117 bp	[1]
β-ENaC	TCCTAGCTTGCCTGTTTGGAA	CAGTTGCCATAATCAGGGTAGAAGAT	79 bp	[2]
γ-ENaC	GCAAGCAATCCTGCAGCTTT	CCCAGGTGAGAACATTCAGCA	102 bp	[3]
renin	GCCTCAGCAAGACTGATTCC	CCTGGCTACAGCTCACAACA	201 bp	[4, 5]
GAPDH	AACGACCCCTTCATTGAC	TCCACGACATACTCAGCAC	191 bp	[6]
Rps13	CCCAGGTCCGTTTTGTGACT	GTGCTTTCGGACAGCAACAG	122 bp	[7]
β-actin	AGCCATGTACGTAGCCATCC	CTCTCAGCTGTGGTGGTGAA	227 bp	[8]

References

1. Wagner CA, Loffing-Cueni D, Yan Q*, et al.* Mouse model of type II Bartter's syndrome. II. Altered expression of renal sodium- and water-transporting proteins. *Am J Physiol Renal Physiol* 2008; **294:** F1373-1380.

2. Fakitsas P, Adam G, Daidie D*, et al.* Early aldosterone-induced gene product regulates the epithelial sodium channel by deubiquitylation. *J Am Soc Nephrol* 2007; **18:** 1084-1092.

3. Lo YF, Yang SS, Seki G*, et al.* Severe metabolic acidosis causes early lethality in NBC1 W516X knock-in mice as a model of human isolated proximal renal tubular acidosis. *Kidney international* 2011; **79:** 730-741.

4. Aoyagi T, Izumi Y, Hiroyama M*, et al.* Vasopressin regulates the renin-angiotensin-aldosterone system via V1a receptors in macula densa cells. *American Journal of Physiology - Renal Physiology* 2008; **295:** F100.

5. Sporková A, Jíchová Š, Husková Z*, et al.* Different mechanisms of acute versus long term antihypertensive effects of soluble epoxide hydrolase inhibition: studies in Cyp1a1-Ren-2 transgenic rats. *Clinical and experimental pharmacology & physiology* 2014; **41:** 1003-1013.

6. Meng Y, Efimova EV, Hamzeh KW*, et al.* Radiation-inducible immunotherapy for cancer: senescent tumor cells as a cancer vaccine. *Molecular therapy : the journal of the American Society of Gene Therapy* 2012; **20:** 1046-1055.

7. Zhang Q, Wang J, Deng F*, et al.* TqPCR: A Touchdown qPCR Assay with Significantly Improved Detection Sensitivity and Amplification Efficiency of SYBR Green qPCR. *PloS one* 2015; **10:** e0132666.

8. Siragy HM, Xue C. Local renal aldosterone production induces inflammation and matrix formation in kidneys of diabetic rats. *Experimental physiology* 2008; **93:** 817-824.